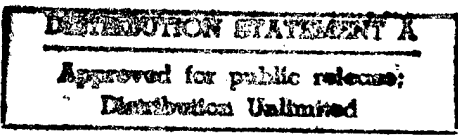


REPORT DOCUMENTATION PAGE			Form Approved OMB No. 0704-0188	
Public reporting burden for this collection of information is estimated to average 1 hour per response, including the time for reviewing instructions, searching existing data sources, gathering and maintaining the data needed, and completing and reviewing the collection of information. Send comments regarding this burden estimate or any other aspect of this collection of information, including suggestions for reducing this burden, to Washington Headquarters Services, Directorate for Information Operations and Reports, 1215 Jefferson Davis Highway, Suite 1204, Arlington, VA 22202-4302, and to the Office of Management and Budget, Paperwork Reduction Project (0704-0188), Washington, DC 20503.				
1. AGENCY USE ONLY (Leave blank)		2. REPORT DATE 4 August 1998	3. REPORT TYPE AND DATES COVERED	
4. TITLE AND SUBTITLE FLIGHT TEST EVALUATION OF A DIFFERENTIAL GLOBAL POSITIONING SYSTEM SENSOR IN RUNWAY PERFORMANCE TESTING			5. FUNDING NUMBERS	
6. AUTHOR(S) Kenneth Paul Germann				
7. PERFORMING ORGANIZATION NAME(S) AND ADDRESS(ES) Mississippi State University			8. PERFORMING ORGANIZATION REPORT NUMBER 98-035	
9. SPONSORING/MONITORING AGENCY NAME(S) AND ADDRESS(ES) THE DEPARTMENT OF THE AIR FORCE AFIT/CIA, BLDG 125 2950 P STREET WPAFB OH 45433			10. SPONSORING/MONITORING AGENCY REPORT NUMBER	
11. SUPPLEMENTARY NOTES				
12a. DISTRIBUTION AVAILABILITY STATEMENT Unlimited distribution In Accordance With AFI 35-205/AFIT Sup 1			12b. DISTRIBUTION CODE	
13. ABSTRACT (Maximum 200 words)				
				
1998 0810 093				
14. SUBJECT TERMS			15. NUMBER OF PAGES 66	
			16. PRICE CODE	
17. SECURITY CLASSIFICATION OF REPORT	18. SECURITY CLASSIFICATION OF THIS PAGE	19. SECURITY CLASSIFICATION OF ABSTRACT	20. LIMITATION OF ABSTRACT	

Name: Kenneth Paul Germann

Date of Degree: December 12, 1997

Institution: Mississippi State University

Major Field: Aerospace Engineering

Major Professor: Dr. Philip D. Bridges

Title of Study: FLIGHT TEST EVALUATION OF A DIFFERENTIAL GLOBAL POSITIONING
SYSTEM SENSOR IN RUNWAY PERFORMANCE TESTING

Pages in Study: 94

Candidate for Degree of Master of Science

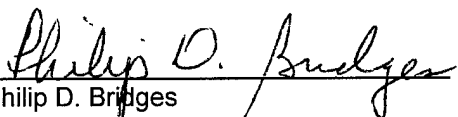
This study discusses the use of a carrier phase differential global positioning system (DGPS) receiver set in basic takeoff and landing performance flight testing. A technique for using DGPS receivers as theodolites in takeoff and landing performance tests is developed. Both position and velocity data are available from a DGPS receiver. As a result distances can be calculated by differencing the position coordinates or by integrating the available ground velocities. Both of these techniques are used and compared to a traditional video theodolite system for ground roll distances. The viability of using DGPS ground speed data in lieu of air data in calculating the distance to clear a barrier is also explored. These methods are used to determine the nominal takeoff and landing performance of an experimental general aviation airplane. Test results are mixed. DGPS velocity integration yields good results for ground phase calculations. All other results are inconclusive.

FLIGHT TEST EVALUATION OF A DIFFERENTIAL GLOBAL POSITIONING
SYSTEM SENSOR IN RUNWAY PERFORMANCE TESTING

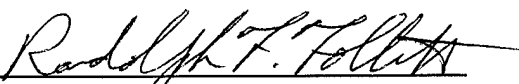
By

Kenneth Paul Germann

Approved:


Philip D. Bridges
Associate Professor of
Aerospace Engineering
(Director of Thesis and Major Professor)


A. George Bennett
Professor of Aerospace Engineering
(Committee Member)


Randolph F. Follett
Assistant Professor
(Committee Member)


John C. McWhorter
Graduate Coordinator of the Department of
Aerospace Engineering


A. Wayne Bennett
Dean of the College of Engineering


Richard D. Koshel
Dean of the Graduate School

DEDICATION

This research is dedicated to my father. His guidance taught me the value critical thinking, impartial evaluation of data, and the scientific method. Without the support he has provided over the years, I would not be the engineer I am today.

ACKNOWLEDGEMENTS

There are so many people whose involvement was critical to completing this project on time. The Department of Aerospace Engineering and RASPET Flight Research Laboratory sponsored my time here, and I am grateful. Joe Cook, Rodney Lincoln, and Ken Ledlow made the completion of the data acquisition system possible. Mr. Ron McGahey and David Novak installed the required systems on the airplane flawlessly. Rani Sullivan provided technical support whenever it was required. Dr. George Bennett provided support every step of the way.

This project also relied heavily on the support of my fellow classmates. Rob Hubbard, Travis Baily, William Maslin, and Andy Ko were up with me at the crack of dawn. The data obtained by them was crucial to the successful completion of my thesis. Shane Creel provided corporate knowledge on the GPS receivers and provided much needed programming support.

Finally, Dr. Philip Bridges provided expertise and support throughout the entire program. He helped maintain the project timeline so that I could graduate on time. I thank him for his time and his patience with me.

TABLE OF CONTENTS

DEDICATION.....	ii
ACKNOWLEDGEMENTS	iii
LIST OF TABLES	vi
LIST OF FIGURES	vii
LIST OF SYMBOLS	ix
CHAPTER	
I. INTRODUCTION	1
II. TAKEOFF AND LANDING THEORY	4
Takeoff Theory	4
Landing Theory	8
III. TAKEOFF AND LANDING PERFORMANCE FLIGHT TESTING	11
Takeoff Performance Flight Test Technique	12
Landing Performance Flight Test Technique	13
Data Requirements	15
Safety Considerations	18
IV. GLOBAL POSITIONING SYSTEM FUNDAMENTALS AND APPLICATIONS ..	19
GPS Satellite Constellation	19
Basic GPS Theory	20
GPS Performance Specifications	21
Differential GPS (DGPS)	22
Sub-Meter Accuracy Through Carrier-Phase Calculations	23
GPS As A Time Space Position Information (TSPI) Source	23
DGPS Used in Lieu of the FAA Approved Del-Norte System	24
V. TEST ITEM DESCRIPTION	26
The NavSymm XR-5M12 GPS Receiver	26
GPS Hardware Configuration For Flight Test	27
GPS Data Post-Processor	28
Manufacturers Kinematic Tests	29
FRRL's Verification Tests	29

CHAPTER	Page
VI. REQUIRED MEASURANDS, APPARATUS, AND CALIBRATION	30
Measuring The Ground Phase	30
Measuring The Air Phase	31
Sensor Calibration	33
VII. TEST EXECUTION	36
Preflight Actions	36
Test Team Actions	37
Standardizing Takeoff Procedures	37
Brake Cooling	38
Standardizing Landing Procedures	38
Postflight Procedures	38
VIII. DATA REDUCTION	39
Spotter and Video Theodolite Data Reduction Methods	39
Air Data System Data Reduction Method	40
GPS Data Reduction	41
Reduction to Standard Day Conditions	43
Algorithm Modifications During GPS System Verification Tests	43
IX. PRESENTATION OF RESULTS	45
GPS Variable Position and Velocity Lag	46
Takeoff Ground Phase Results	50
Takeoff Air Phase Distance Results	55
Takeoff Position and Velocity Profiles	56
Landing Air Phase Distance Results	58
Landing Ground Phase Distance Results	59
Landing Position and Velocity Profiles	61
X. CONCLUSIONS AND RECOMMENDATIONS	63
FUTURE STUDIES	63
REFERENCES CITED	65
APPENDIX	67

LIST OF TABLES

TABLE		Page
2.1	Typical Coefficients of Rolling Friction For Aircraft During Takeoff Roll	5
3.1	Percent Increase of Takeoff Distance With Increasing Density Altitude	11
4.1	GPS Accuracies	21
9.1	Takeoff Ground Distance Calculation Statistics for Flight GPS-04	53
9.2	Takeoff Ground Distance Calculation Statistics for Flight GPS-05	53
9.3	Takeoff Ground Roll Calculation Error Statistics From All Flights	54

LIST OF FIGURES

FIGURE		Page
2.1	The Phases of Takeoff and Landing	4
2.2	Free Body Diagram of an Aircraft on the Ground	5
2.3	Forces During the Takeoff Ground Roll	7
2.4	Forces Acting on Aircraft During the Landing Roll	10
3.1	Video-Theodolite Runway Configuration	16
4.1	Satellite Triangulation Used In the Global Positioning System	20
4.2	Graphical Summary of GPS Error Sources	22
4.3	Reverse Triangulation of DGPS	22
6.1	Video-Theodolite Geometry at Starkville-Bryan Field	31
6.2	Rosemount Airspeed Transducer Calibration Model: 1221D1B1 S/N: 53	34
6.3	Rosemount Altitude Transducer Calibration Model: 1241A4BCD S/N: 345	35
8.1	Vertical Speed Comparison from Takeoff No. 10	44
9.1	GPS and DAS Vertical Speed Profiles for Takeoff No. 7	47
9.2	Position Time Lag History For Flight GPS-05	48
9.3	Takeoff Ground Phase Distance Measurements	51
9.4	Error of Ground Roll Calculations	52
9.5	History of Position and Velocity Difference Between Integration and Position Techniques	55
9.6	Air Distance Calculations for Flight GPS-05	56
9.7	Position and Velocity Profiles for Takeoff No. 11	57
9.8	Altitude and Vertical Velocity Profiles for Takeoff No. 11	58

FIGURE		Page
9.9	Landing Air Phase Distance Results for Flight GPS-05	59
9.10	Landing Ground Phase Distance Results	60
9.11	Distance and Velocity Profiles for Landing No. 11	61
9.12	Altitude and Velocity Profiles for Landing No. 11	62

LIST OF SYMBOLS

Φ	Runway Slope
β	Crosswind Angle
α	Angle of Attack
ρ	Air Density
μ_B	Coefficient of Braking Friction
μ_R	Coefficient of Rolling Friction
a	Acceleration
AFB.....	Air Force Base
AGL.....	Above Ground Level
$C_{L_{\text{liftoff}}}$	Lift Coefficient at Liftoff
D	Drag
DGPS.....	Differential Global Positioning System
D_L	Drag During Landing Roll
DOD.....	Department of Defense
E_{BR}	Easting Coordinate At Brake Release
EGT.....	Exhaust Gas Temperature
E_{LO}	Easting Coordinate At Liftoff
FAA.....	Federal Aviation Administration
FAR.....	Federal Aviation Regulations
FTE.....	Flight Test Engineer
g	Acceleration Due to Gravity
GPS.....	Global Positioning System
H_i	Indicated Altitude
INS.....	Inertial Navigation System
KTAS.....	Knots True Airspeed
L	Lift
L_L	Lift During Landing Roll
m	Mass
MSL.....	Mean Sea Level
n.m.....	Nautical Miles
NAS.....	Naval Air Station
N_{BR}	Northing Coordinate At Brake Release
N_{LO}	Northing Coordinate At Liftoff
psi.....	Pounds per Square Inch
RFRL.....	Raspert Flight Research Laboratory
S	Wing Area
S_A	Air Phase Distance
S_G	Ground Phase Distance
S_{G1}	Stabilized Ground Phase Distance
S_{G2}	Flare Ground Phase Distance
S_{LND}	Total Landing Distance
S_{TO}	Total Takeoff Distance
T	Thrust

t.....	time
T _j	Measured Outside Air Temperature
T _L	Thrust During Landing Roll
t _f	Time Spent in Flare
TSPI.....	Time Space Position Information
USAF.....	United States Air Force
V.....	Aircraft Velocity
V _{BH}	Velocity at Barrier Height
V _{eco}	Equivalent Airspeed During Climbout
V _{ehco}	Horizontal Component of Climbout Equivalent Airspeed
V _G	Ground Speed
V _i	Indicated Velocity
V _L	Velocity During Landing Roll
V _{liftoff}	Aircraft Velocity at Liftoff
V _{rot}	Aircraft Velocity at Rotation
V _{TD}	Velocity at Touchdown
V _W	Wind Velocity
W.....	Aircraft Gross Weight

CHAPTER I

INTRODUCTION

Every flight of every aircraft built has to begin with a takeoff and end with a landing. Ward provide the following definitions.

"Takeoff is the process by which an airplane is brought from a standstill to a safe flight condition. Landing is the process by which an airplane is brought from a safe flight condition to a standstill."¹

The time, distance from liftoff or to touch down, and the ground roll distance are dependent on many factors. The aircraft gross weight, the pressure altitude, the wind speed, and ambient temperature are some of the most important. Quantifying how these variables affect takeoff and landing distances is very important to both the aircraft manufacturer and to the operational aircrew. The manufacturer must know whether his aircraft can meet or exceed the regulatory standards. Daily, the operational aircrew must be able to easily determine what these distances are in order to know if a given airfield is long enough for standard operations. In the case of short field and emergency engine-out operations, it is very important to have a good understanding of the aircraft performance.²

The only reliable way of obtaining this data accurately for a new or modified airplane is to take it out to the runway and perform many takeoffs and landings. These tests are designed to measure both the distance covered on the ground and the distance covered in the air during each maneuver. The distances covered are highly susceptible to pilot technique. Despite efforts to standardize pilot techniques, they will never be uniform. Therefore, it is impossible to exactly measure takeoff and landing distances, and elementary statistical methods must be

employed over several samples.¹ The higher the number of samples (takeoffs and landings) performed, the higher the risk. Takeoff and especially landing tests are statistically the most hazardous. According to Ward, they are not for the faint of heart:

"Takeoff and landing tests are some of the most dangerous tests conducted in certifying an airplane. They require the flight test crew to establish flight envelope limits (and thus occasionally exceed them!) while on or very close to the ground with the airplane in its least controllable configuration. And that is where most accidents occur."¹

These tests must be performed, however. The entire flight test team must approach these tests with extensive planning and strict flight discipline. Although this report focuses on normal takeoffs and landings, a complete flight test program will also include refused takeoffs, cross-wind operations, wet/icy runway operations, barrier tests, and engine-out operations.

The most difficult aspect of performing take-off and landing tests is collecting the distance data. Traditional measurement methods range from the inexpensive and simple to the costly and complex. Unfortunately, accuracy is directly proportional to expense. The simple methods use people or simple theodolites for distance measuring. These methods do not provide very high accuracy and require much manpower. More highly accurate methods require laser or radar tracking equipment that is expensive and is not readily available. On board accelerometer packages can also be used but are also very expensive.

On April 27, 1995 the U.S. Space Command declared that the Global Positioning System (GPS) was fully operational. The system includes a constellation of 24 NavStar satellites orbiting the earth in 12 hour orbits. There are six equally spaced orbital planes inclined at about fifty-five degrees. These satellites continuously broadcast signals to terrestrial receivers. The receivers can then calculate their position on earth. Originally, GPS accuracies were advertised to be approximately 100 meters and are usually even more accurate. Technological

improvements since 1995 have improved these accuracies considerably. As a result these systems are being implemented in a variety of flight test applications.³

The Raspet Flight Research Laboratory recently purchased a highly accurate GPS receiver and processing system with advertised sub-meter accuracy. This system should be perfect to use as a tracking system for flight test applications. Since GPS is proven to work well in steady-level flight applications, a more rigorous test of this system is in order. Due to the large accelerations involved, the troublesome area of takeoff and landing distance measurements is a perfect area to test this new system and its effectiveness as a tracker. A good GPS system can provide an exact position history of a maneuver. Additionally, GPS provides a ground speed history. Takeoff and landing distances should then be available through two methods. Differencing the locations of brake release, liftoff, touchdown, full stop, and 50 foot points should provide a direct solution to the distances covered. Integrating the velocity profiles should give us approximately the same solution. The solutions gained through utilizing GPS should correlate with those gained through traditional methods.

CHAPTER II

TAKEOFF AND LANDING THEORY

In conducting takeoff and landing tests, it is important to understand all of the forces at work. During these maneuvers, all of the aerodynamic forces are constantly changing. Additionally, there are frictional forces acting on the airplane that are functions of the changing aerodynamic forces. This flight regime is complicated and difficult to model. The following discussion shows how these forces interact during both the takeoff and landing.

Takeoff Theory

Each takeoff and landing is divided into two phases: the ground phase and the air phase. The ground phase of the takeoff (S_G) begins at brake release and ends when the airplane lifts off the surface. The air phase (S_A) begins at lift-off and continues to the barrier height. The barrier height is defined as 50' for military and light civil aircraft, 35 feet for heavy civil aircraft¹. Figure 2.1 shows this geometry.

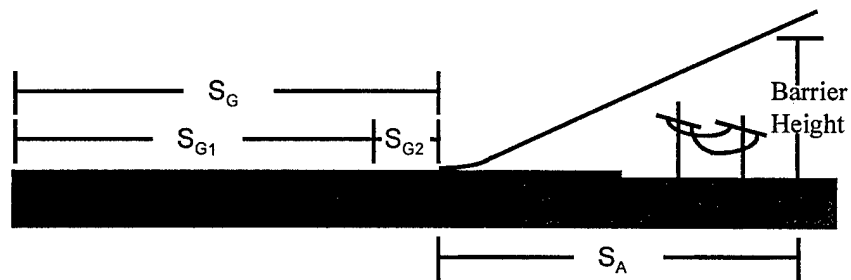


Figure 2.1: The Phases of Takeoff and Landing

There are a large number of factors which affect the length of the ground run. As a result, it is impractical to model it completely. To simplify the analysis, Ward recommends including only the following major influences:¹

Gross Weight
 Thrust Available
 Ambient temperature
 Pressure altitude
 Wind Direction and Velocity
 Runway Slope
 Coefficient of Friction

To simplify the analysis, we will also assume that the ground run ends at the moment of rotation and will be designated S_{G1} . Rotation is considered separately and designated S_{G2} . Figure 2.2 is a free-body diagram showing the forces acting on an aircraft during the initial ground run, S_{G1} . The forces are defined in the usual sense. Lift opposes weight and thrust opposes drag, rolling friction, and runway slope effects.

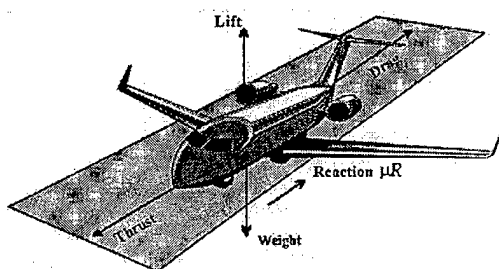


Figure 2.2: Free Body Diagram of an Aircraft on the Ground²

Table 2.1: Typical Coefficients of Rolling Friction For Aircraft During Takeoff¹

SURFACE	RANGE FOR μ
Concrete	.02-.03
Hard Turf or Short Grass	.05
Long Grass	.10
Soft Ground	.10-.30

Typical values for runway friction coefficients are given in Table 2.1. Runway slope produces a weight (W) component parallel to the runway ($W \sin \Phi$) and a small reduction in normal force ($W \cos \Phi$). Since the maximum runway slope is typically 3%, these forces can be simplified by assuming small angles.

With this assumption, the horizontal component becomes $W\Phi$ and the vertical component becomes merely W . Resolving the free body diagram results in:

$$F = ma = T - D - \mu(W - L) - W\Phi \quad (2.1)$$

Wind effects are also important. The headwind speed is given by $\pm V_w \cos|\beta|$, where β is the wind angle and a positive sense is a tailwind. Using this analysis, the aircraft velocity is:

$$\frac{dS_{G1}}{dt} = V \pm V_w \cos|\beta| \quad (2.2)$$

Since $a = \frac{dV}{dt}$, it can be solved for dt to yield $dt = \frac{dV}{a}$. Equation 2.2 becomes

$$dS_{G1} = (V \pm V_w \cos|\beta|) \frac{dV}{a} \quad (2.3)$$

which is integrated to yield an exact solution for the ground run, providing a , V , and V_w are known throughout the takeoff roll and V_{liftoff} can be determined. This equation is:

$$S_{G1} = \int_0^{V_{\text{rot}}} \frac{(V \pm V_w \cos|\beta|) dV}{a} \quad (2.4)$$

By substituting the basic force equation (2.1) into this equation, we have a new expression in which all the variables are known or can be measured for a given aircraft.¹ This final equation is shown below with the takeoff limits of integration, where the velocity at brake release is 0, and the velocity at rotation is V_{rot} .

$$S_{G1} = \int_0^{V_{\text{rot}}} \frac{W(V \pm V_w \cos|\beta|) dV}{g[T - D - \mu(W - L) - W\Phi]} \quad (2.5)$$

Note that $\Phi > 0$ for uphill takeoffs. This equation will provide an exact solution to S_G provided these values can be measured or predicted directly or indirectly throughout the takeoff ground run.

The rotation distance should be calculated separately. As the aircraft rotates, the angle of attack (α) increases and lift increases with α and V . The increasing lift component affects the friction force, the drag force, and the runway slope force in a non-linear fashion. It is easier to assume an instantaneous change in α and to ignore $W\Phi$ during rotation. Ward simplifies this calculation further by assuming an average time to rotate (t_r), typically 3 to 4 seconds.¹ Also, assume the average velocity during rotation to be V_{liftoff} . Using these assumptions, the following equation is gained for the rotation distance, S_{G2} :

$$S_{G2} = t_r V_{\text{liftoff}} = t_r \sqrt{\frac{W}{\frac{1}{2} \rho S C_{L_{\text{liftoff}}}}} \quad (2.6)$$

The resulting total ground roll distance is

$$S_G = S_{G1} + S_{G2} \quad (2.7)$$

Figure 2.3 shows the typical force profiles during takeoff. The actual magnitudes of these forces drives the actual distance required for the ground roll.

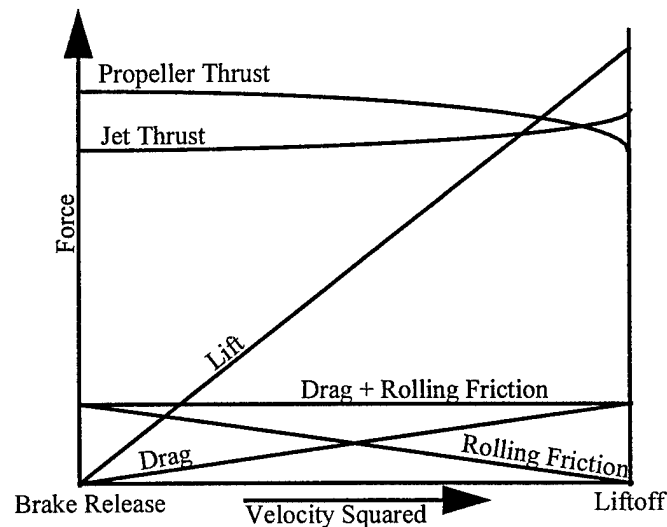


Figure 2.3: Forces During the Takeoff Ground Roll²

The air phase begins at liftoff and ends when the airplane reaches the barrier height. The ground distance covered during this phase, S_A , can be found using the energy method. The energy equation for S_A and a 50 foot barrier height is:²

$$\int_0^{S_A} (T - D) ds = \frac{W}{2g} (V_{BH}^2 - V_{liftoff}^2) + 50W \quad (2.8)$$

where V_{BH} is the climbout velocity at barrier height. This is usually mandated to be at least $1.3V_{s1}$, where V_{s1} is the power off stall speed in the takeoff configuration. Integrating equation 2.8 yields the following approximation for S_A :²

$$S_A = \frac{W}{(T - D)_{avg}} \left[\frac{V_{BH}^2 + V_{liftoff}^2}{2g} + 50W \right] \quad (2.9)$$

The assumption that T-D is constant throughout the climbout is not very good. The errors introduced by this assumption remain small if the time involved in the climbout is small or the aircraft can transition quickly to V_{BH} .

The ground phase and the air phase combine to establish the total distance required to takeoff and clear an obstacle.

$$S_{TO} = S_G + S_A \quad (2.10)$$

Landing Theory

The landing is divided into a ground and air phase as well. The air phase begins at the barrier height with a constant rate of descent or a constant descent angle and ends when the aircraft touches the runway. The ground phase begins at touchdown and continues until the aircraft comes to a complete stop. Like takeoff, it is impossible to model the landing completely. The analysis of the landing depends on the same factors as takeoff and is very similar.

The air phase of the landing can be developed from the energy equation in the same manner that takeoff is developed. The energy equation for the landing air phase is

$$\int (T - D) ds = \frac{W}{2g} (V_{TD}^2 - V_{BH}^2) - 50W \quad (2.11)$$

This equation, when integrated, yields²

$$S_A = \frac{-W \left(\frac{V_{TD}^2 - V_{BH}^2}{2g} \right) - 50W}{(T - D)_{avg}} \quad (2.12)$$

The distance covered during the landing flare is found similarly to the takeoff rotation. However, on landing it is only valid if minimum aerodynamic braking is used and the aircraft is rotated to the landing attitude as quickly as practical. This can be considered to be 3 to 4 seconds. When these assumptions are met, equation 2.6 be a reasonable approximation of S_{G1} . Otherwise a more rigorous investigation is possible using equation 2.13.¹

The development of the ground roll equation is identical to that of the takeoff. The terms have substantially different effects, however. The acceleration during the landing roll is negative. With the power at idle, the engine creates very little thrust. When thrust reversers are used, the thrust term is negative, contributing significantly to the deceleration. The coefficient of braking friction, μ_b , is significantly higher than the coefficient of rolling friction. It ranges from .2 on ice to .7 on dry concrete.¹ In many aircraft, aerodynamic braking is employed by remaining at a high pitch attitude for a portion of the ground roll. Aerodynamic braking devices such as speed brakes or a drag chute are often employed, making the aerodynamic forces contribute significantly to the deceleration.¹ The ground roll equation for landing is then

$$S_{G2} = \int_0^{V_{rot}} \frac{W(V_L \pm V_W \cos|\beta|) dV}{g[T_L - D_L - \mu(W_L - L_L) - W_L \Phi]} \quad (2.13)$$

Figure 2.4 shows the typical force profiles for a landing roll. The actual magnitudes of these forces drives the actual roll-out distance.

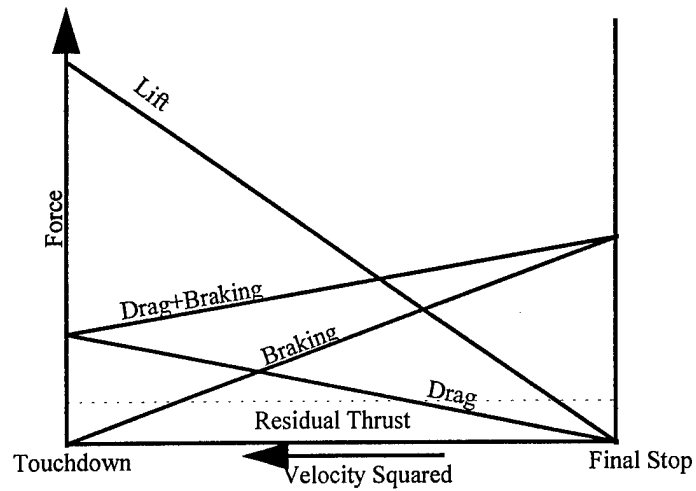


Figure 2.4: Forces Acting on Aircraft During the Landing Roll²

The total distance required to land over an obstacle can be calculated by

$$S_{LND} = S_A + S_{G1} + S_{G2} \quad (2.14)$$

CHAPTER III

TAKEOFF AND LANDING PERFORMANCE FLIGHT TESTING

The theoretical equations are a good method of obtaining estimates of the takeoff and landing performance of an aircraft. The equations incorporate several assumptions and cannot predict the performance exactly, even if all the parameters of the equations can be accurately obtained. According to Ward, the best estimate that can be gained through a rigorous application of these equations is 5%.¹ Results can be much worse. For this reason, both the FAA and the military require that takeoff and landing performance be demonstrated. Both organizations have even established minimum standards of performance which must be met for certification. The performance data in the pilots operating handbook must also be based on flight test data. This must include the anticipated effects of runway surface, runway slope, and density altitude.² Table 3.1 shows how takeoff and landing distances are affected by changes in density altitude.

Table 3.1: Percent Increase of Takeoff Distance With Increasing Density Altitude²

Density Altitude	Supercharged Reciprocating Engine	High Thrust to weight Turbojet	Low Thrust to Weight Turbojet
Sea Level	0	0	0
1000 ft	3	6.1	9.8
2000 ft	6.1	12.5	19.9
3000 ft	9.3	19.5	30.1
4000 ft	12.6	26.4	40.6
5000 ft	16.1	34.7	52.3
6000 ft	19.7	43.2	65.8

Takeoff and landing tests are largely affected by factors that cannot be accounted for such as variations in pilot technique. It is possible to estimate the capabilities of the airplane only within broad limits, relying on statistical averaging of many takeoff and landing maneuvers to cancel residual errors.⁴

Since statistical methods will be used to determine the approximate air and ground distances, we must know the number of samples required. When pilots are using a standardized technique, the scatter in S_G is about 4%. Probability calculations show that to have 95% confidence level of being within 5% of the true distance, at least 5 measurements must be made. This can be increased to 2.5% accuracy if the number of samples is increased to 6. Additional runs will reduce the measurement precision required. It is recommended by Ward that at least 6 takeoffs and landings be accomplished for each configuration.¹

Takeoff Performance Flight Test Technique

Takeoff tests are conducted to find the time, airspeed to rotation, distance to lift-off, and distance to clear a minimum barrier height for a range of gross weights and flap settings.⁵ The first objective of these tests is to document reliable and repeatable takeoff data that can be used by the pilot under normal and emergency conditions. Both military and FAA specifications require that takeoff performance data be presented to pilots in a manner such that the aircraft may be safely operated in various combinations of gross weight, density altitude, runway length, runway slope, runway condition and winds. The second objective of these tests is to comply with regulatory requirements. The following is a discussion of the FAA requirements for certification of aircraft under Federal Aviation Regulations (FAR) part 23. Part 23.53 paragraph (b) states of takeoff performance:

"For normal, utility, and acrobatic category airplanes, the distance required to takeoff and climb to a height of 50 feet above the takeoff surface must be determined for each weight, altitude, and temperature within the operational limits established for takeoff with--

- (1) Takeoff power on each engine;
- (2) Wing flaps in the takeoff position(s); and
- (3) Landing gear extended."⁶

The flight test technique used in takeoff performance testing is fairly simple. The pilot flies several static takeoffs using normal or short field techniques in all desired configurations.

Since pilot landing techniques vary widely, standardizing the pilot techniques used is very important. USAF Test Pilot school recommends standardizing the following:⁴

1. Throttle setting prior to brake release
2. Throttle technique at/immediately after brake release
3. Control positions during acceleration
4. Airspeed at rotation
5. Rate of rotation
6. Aircraft attitude at liftoff
7. Gear and flap retraction points

Landing Performance Flight Test Technique

Landing tests are conducted to find the time, distance from a minimum barrier height to touchdown, and distance from touch-down to full-stop for a range of gross weights and flap settings. The first objective of these tests is to document reliable and repeatable landing distance data that can be used by the pilot under normal and short field conditions. Both military and FAA specifications require that landing performance data be presented to pilots in a manner such that the aircraft may be safely operated in various combinations of gross weight, density altitude, runway length, runway slope, runway condition and winds. The second objective of these tests is to comply with regulatory requirements. The following is a discussion of the FAA requirements for certification of aircraft under FAR part 23. Part 23.57 states of landing distance performance:

"The horizontal distance necessary to land and come to a complete stop from a point 50 feet above the landing surface must be determined, for standard temperatures at each weight and altitude within the operational limits established for landing, as follows:

- (a) A steady approach at not less than VREF, determined in accordance with Sec. 23.73 (a), (b), or (c), as appropriate, must be maintained down to the 50 foot height and--
 - (1) The steady approach must be at a gradient of descent not greater than 5.2 percent (3 degrees) down to the 50-foot height.
 - (2) In addition, an applicant may demonstrate by tests that a maximum steady approach gradient steeper than 5.2 percent, down to the 50-foot height, is safe. The gradient must be established as an operating limitation and the information necessary to display the gradient must be available to the pilot by an appropriate instrument.
- (b) A constant configuration must be maintained throughout the maneuver.
- (c) The landing must be made without excessive vertical acceleration or tendency to bounce, nose over, ground loop, porpoise, or water loop.
- (d) It must be shown that a safe transition to the balked landing conditions of Sec. 23.77 can be made from the conditions that exist at the 50 foot height, at maximum landing weight, or at the maximum landing weight for altitude and temperature of Sec. 23.63 (c)(2) or (d)(2), as appropriate.
- (e) The brakes must be used so as to not cause excessive wear of brakes or tires."⁶

The flight test technique used in landing performance testing is fairly simple. The pilot flies several landings using normal or short field techniques in all desired landing configurations. Since there is a wide variation in pilot techniques, it is very important to standardize the techniques used. It is most important to standardize the following aspects of the landing.⁴

1. Power handling during approach, flare, and touchdown
2. Attitude of flare initiation
3. Rate of rotation in flare
4. Length of hold-off time
5. Touchdown speed
6. Rapidity of initiation of braking
7. Use of drag chute and/or thrust reversers
8. Brake pedal pressure

Data Requirements

Test measurements must be taken to determine the ground run distance, liftoff airspeed, and the velocity/acceleration profiles during both phases.¹ Takeoff and landing performance involves accelerations and decelerations. The measurement of these dynamic conditions can be difficult. Data requirements are often broken down into two categories: external data and internal data.⁴ External data is the data external to the airframe and powerplant combination. External measurands include; ground roll, distance to barrier height, ground speed and accelerations, runway temperature, ambient pressure and the wind velocity. Internal data includes the engine power output parameters, airspeed, altitude, ambient temperature, and exhaust gas temperature (EGT). The methods of measuring the internal parameters with on-board instrumentation are well established. However, the measurement of the distance, velocity, and acceleration profiles has traditionally been troublesome. There are many ways to collect and process this data involving both on-board and external measurements. The following is a discussion of several of these methods. Notice they are increasingly more complicated and expensive. However, the increased complexity and expense usually yields increased accuracy.

The most basic method of measuring the takeoff distance is direct external position measurements. For example, observers placed near the anticipated liftoff point can mark that point as the aircraft goes by. This is a good idea no matter which method is used. The data collected by these observers can be used as a check for the data obtained from other sources.⁷ The U.S. Air Force Academy found that using a surveyors transit can be used to find the ground distance with good results.⁸ A variation on the transit is using phototheodolites. These are cameras with a calibrated azimuth scale, allowing postflight analysis. Phototheodolites with both an azimuth and elevation scale can be used to obtain both the ground and the air distance. Phototheodolites can be as accurate as ten feet. Differentiation will then yield the velocity and acceleration profiles.⁴

Obtaining the azimuth scale when using standard home video tape cameras can be a problem. The USAF Flight Test Engineering Handbook recommends putting equally spaced markers along the runway.⁷ After carefully choosing the camera location, these markers can be used as a calibrated azimuth scale. Figure 3.1 shows this geometry.

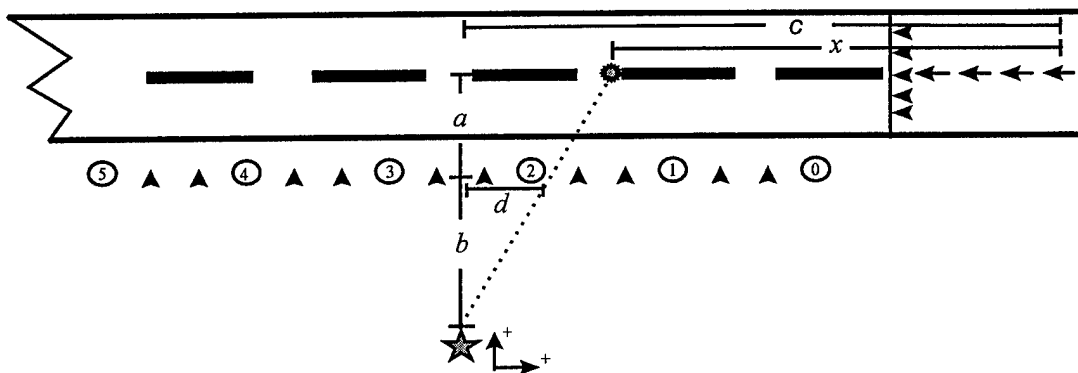


Figure 3.1: Video-Theodolite Runway Configuration

Equation 3.1 can then be used to find the event position on the runway

$$x = c - \frac{(a+b)d}{b} \quad (3.1)$$

where a is the distance from the centerline to the markers, b is the distance from the markers to the camera, c is the centerline distance from the runway origin to the camera line, d is the distance from the camera site to the apparent marker position, and x is the distance from the runway origin to the event point.

If an elevation scale is not available, these methods do not work very well in measuring the air distance. Radio altimeters can be used. The National Test Pilot School suggests an inexpensive solution to this problem.² The pilot lifts off at the climbout indicated velocity. The climbout indicated airspeed and vertical velocity are recorded. The climbout airspeed can then be converted to equivalent airspeed, V_{eco} . Using geometry, V_{eco} and the climb rate can be used

to find the horizontal velocity component, V_{ehco} . V_{ehco} is multiplied by the time required to reach the barrier height to yield the total air distance.

The most expensive method of external tracking utilizes very precise theodolites. Cinetheodolites are similar to phototheodolites. They use high-speed motion picture cameras placed on accurately surveyed sites to triangulate the exact positions and velocities. Three cameras are required to triangulate horizontal and vertical positions. The film will often run out or break at an inopportune moment. Therefore, it is recommended that four cameras be used. These systems are typically found at major flight test centers (i.e. Yuma proving grounds, Edwards AFB, NAS Patuxent River) and the aircraft must be taken to these facilities. This may not always be feasible.

A similar tracking system uses radar beacons or tracking lasers. Many of these systems are nearly as accurate as cine-t's, and only require one tracker to resolve all three positions. This reduces the cost of these system over cine-T's, but they are still expensive. The FAA approved measuring device is the Del-Norte device.⁹ This system is based on an X-band radar transponder. It consists of a ground based telemetry sub-system and an air-based beacon subsystem. It provides direct position measurement, but does not provide any velocity or altitude information.

There are several methods of getting takeoff and landing distances from on-board instrumentation. Modern accelerometers such a those found in inertial navigation platforms accurately record the acceleration profile throughout the maneuver. The acceleration profile is integrated to gain the velocity and position profiles. If a continuous record of airspeed data is available, it can also yield the velocity profile.¹ This requires that the position and instrument error corrections are known for the installed instrumentation system.

Determining the exact point of liftoff or touchdown is difficult. Direct measurement of this parameter is preferred. Event markers, triggered by the extension of the landing gear struts,

are the most accurate way of determining the liftoff/touchdown points. This can be obtained from a weight-off-wheels switch, often found on retractable gear aircraft. Less directly, the first occurrence of vertical velocity in the takeoff data record can be used as well. Least accurate is a radio call from the pilot or observers annotating the liftoff time with an external clock.

Safety Considerations

Safety is paramount when conducting these tests. The aircraft is being operated in its most precarious flight regime: low airspeed, high angle of attack, and close to the ground. There is little margin for error and, as a result, these tests are considered hazardous. When a sortie is being dedicated to landing tests, it is also important to consider brake energy in the planning. Elevated brake temperatures can result in overheated braking systems or even fire. Takeoff and landing tests should be approached with cautious and meticulous planning.

CHAPTER IV

GLOBAL POSITIONING SYSTEM FUNDAMENTALS AND APPLICATIONS

The Global Positioning System (GPS) is a satellite navigation system developed and operated by the US Department of Defense (DOD). The system permits land, sea, and airborne users to determine their three dimensional position, velocity, and time. It is available globally, around the clock, and in all weather conditions. GPS uses the 24 NAVSTAR (NAVigation Satellite Timing and Ranging) satellites. The constellation configuration allows a receiver to be within view of 4 to 12 satellites at any time. A minimum of 4 satellites is required to resolve latitude, longitude, altitude (referenced to Mean Sea Level, MSL) and GPS time.³

GPS Satellite Constellation

The NAVSTAR constellation consists of 24 satellites, 21 operational and 3 active spares. Each satellite orbits the earth at 10,898 n.m. in one of six 55° orbital planes. Each plane contains four satellites. The period of each satellite is approximately 12 hours.¹⁰ The satellites simultaneously broadcast time and position information which the receivers use for solution resolution. The satellites are identified by a pseudo-random (PRN) code within the signal. GPS signal strengths are low, and the code is used by the receiver to pull the signal from the noise. The constellation broadcasts on two L-band frequencies. L1 is at 1.57542 GHz and contains two codes, the coarse/acquisition (C/A) and precision (P) codes. L2 is at 1.22760 GHz and contains only P code which is encoded for military use. Civilian users can only access the unencrypted C/A code.¹

Basic GPS Theory

The system uses satellite signals to triangulate a receiver's position on the earth. Signals are sent out by every satellite in the constellation at predetermined times. The signals are digitally encoded to identify each satellite. The earthbound receiver receives this signal and determines the phase shift in the code. This phase shift is a result of the signal travel time, and accordingly, the approximate distance to the satellite is known. This approximate distance is called pseudo-range. Receivers are equipped with the satellite position data. The receiver's data is continually updated with satellite ephemeris data broadcasted to the receiver by the satellites. The ephemeris data includes minor orbital corrections that are a result of the Earth's non-spherical gravitational field and solar and lunar gravitational effects.³ Finally, with the positions of three satellites and the distances to these satellites known, an approximate position is found. Figure 4.1 shows how this works.

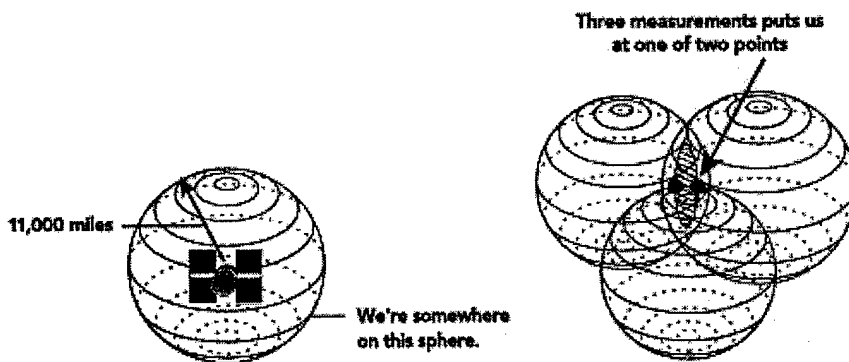


Figure 4.1: Satellite Triangulation Used In the Global Positioning System³

A pseudo-range from one satellite resolves to the surface of a sphere. Two pseudo-ranges from two satellites results in two intersecting spherical surfaces. Two intersecting spherical surfaces resolve the solution to a circle. Three satellite spherical surfaces will resolve to two points. One of these two points is an unreasonable solution and is discarded. After a fourth satellite measurement is taken, it may not resolve to the same point. This happens when

the receiver clock is not synchronized to the highly accurate atomic clocks carried on the satellites (universal time). The receiver then searches for a timing offset which will allow the four spheres to resolve to a single point. The receiver's clock is then resynchronized with universal time and applies the correction to the remaining measurements. The receiver continues to compensate whenever a clock discrepancy is found.³

GPS Performance Specifications

The following table summarizes the relative accuracy of the system.

Table 4.1: GPS Accuracies¹¹

Parameter	P-code Accuracy	C/A-code Accuracy	D-GPS
Horizontal Position	17.8 m	30-100 m	1.5 m
Vertical Position	27.7 m	156 m	3.4 m
Horizontal Velocity	.1 m/s	Not Available	N/A
Vertical Velocity	.2 m/s	Not Available	N/A
Time Accuracy	100 ns	167 ns	Code dependent

The numbers presented are worst-case. Under normal circumstances these values are substantially better. There are several sources of error driving the relative accuracy of the system.

1. Bias errors from Selective Availability (SA) encoding are the primary differences between P and C/A code accuracy. SA is the DOD's intentional degradation of the C/A-code signals. This is done by dithering the clock signals, where the P-code signals are undithered. This process degrades the C/A code accuracy to 30-100 m.
2. Other bias errors are less significant. These include satellite clock errors, ephemeris data errors, multi-pathing, tropospheric delays, ionospheric delays. Figure 4.2 illustrates the effects of these errors.
3. Noise errors from either PRN background noise or internal receiver noise.

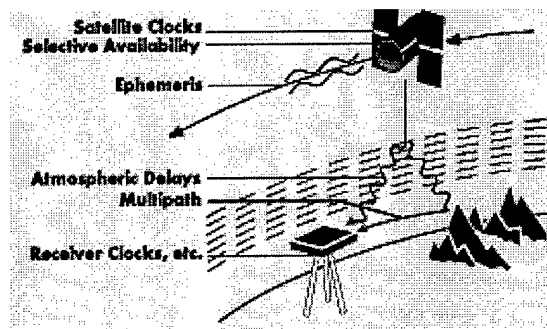


Figure 4.2: Graphical Summary of GPS Error Sources³

Differential GPS (DGPS)

These errors can be compensated for through a differential system known as DGPS. A GPS receiver is placed at a surveyed point on the earth. Instead of using the timing signals to calculate its position, it uses its known position to calculate timing. It figures out what the timing should be, compares it to the actual timing, and calculates the correction.³ The reference station computes the corrections for each satellite within view, and broadcasts these corrections. A DGPS receiver receives these corrections and incorporates them into its solution. This method essentially compensates for the SA dithering, and therefore improves the C/A accuracy to the P-code accuracy. Stand-alone DGPS achieves accuracies to 3-10 meters. Figure 4.3 illustrates the DGPS system operation.

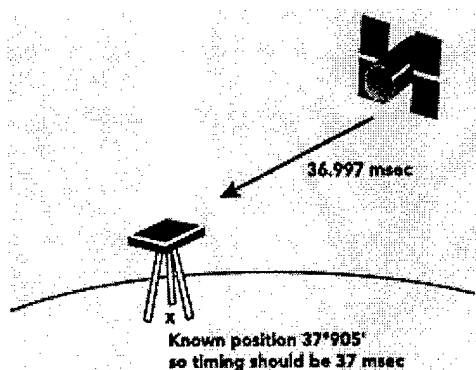


Figure 4.3: Reverse Triangulation of DGPS³

A DGPS system integrated with an inertial navigation system (INS) can achieve up to 1.5 m accuracies. Many of the newest systems (including non-INS coupled) are claiming even better performance.

Sub-Meter Accuracy Through Carrier-Phase Calculations

Code-Phase GPS receivers use the pseudo-random code as a baseline, aligning the code and calculating the phase shift. This code operates at approximately 1MHz overlaid on a 1.6 GHz carrier frequency. Modern code-phase receivers can calculate position to within 2% of the wave-length.³ This corresponds to 3-6 meters maximum performance. However, if the carrier-phase of the GPS code is utilized, 2% of the wavelength is less than a centimeter. In reality, these methods are used in conjunction with each other. The code-phase method is used to get close, then the carrier phase method is used to resolve the solution. Notice that if the code phase resolves the solution to even 1m, there are now 100 cycles remaining to resolve. This is known as the "carrier-phase ambiguity" and is currently the most daunting problem facing GPS engineers.³ As the processors and the algorithms get more precise, accuracy of these systems will increase.

GPS As A Time Space Position Information (TSPI) Source

In order to quantify GPS' utility as a TSPI source it must be compared against existing TSPI sources and evaluated for accuracy. McClellan AFB, CA has performed such testing. They used GPS system in conjunction with high accuracy cinetheodolites (cine-t's) on F-111 Pacer Strike aircraft.¹²

The cine-t system used is the 4-camera system at Edwards AFB, CA. This system has a spherical root-mean-square (RMS) position accuracy of 14.5 ft and velocity accuracy of 2.3 ft/sec. The GPS system used was a carrier phase P-code system DGPS system at 1 Hz. This

system was reported by Holloman AFB to have a spherical RMS position accuracy of 6 ft and a velocity accuracy of .3 ft/sec.¹²

The systems were compared in straight and level flight, a 1.5 g descending turn at 330 KTAS from 7000 AGL to 5500 AGL, and a 4g pull-up at 540 KTAS to 45°. In performing comparisons, cine-t data is considered as the truth source. During 1 g flight both position and velocity GPS data was within the error bounds of the cine-t data. The spherical deviations from cine-t data were 6.8 RMS in position and .55 ft/sec in velocity. During the descending turn, the GPS position was within the cine-t RMS accuracy. The spherical deviation was 7.6 ft RMS. The GPS velocity data did not perform as well. It varied considerably, averaging 1.2 ft/sec RMS but was as high as 2.3 ft/sec. During the 4g pull-up, position varied as much as 10 ft in horizontally and 16 feet in altitude. The overall RMS position accuracy was still within the cine-T RMS. The spherical position RMS was 8.3 ft. The velocity varied widely, especially at the beginning of the pull-up. The overall velocity RMS deviation was 1.9 ft/sec but was 2.3 ft/sec at the beginning of the pull-up.

The PACER Strike team concluded that this was extremely good correlation especially since DGPS is 10% of the cost of cine-t data. However, they did express concerns over the velocity errors during accelerated flight. They recommended that the system be used for moderate maneuvering only.

DGPS Used in Lieu of the FAA Approved Del-Norte System

Israel Aircraft Industries (IAI) recently performed a comparison of the FAA approved Del-Norte X-Band transponder system to a NovAtel code phase DGPS system during takeoff and landing tests. Their data shows that the DGPS system performance is superior to the transponder system in horizontal distance and velocity.⁹ However the altitude performance is worse. The author suggests that carrier-phase processing would effectively eliminate this problem.

RFRL has purchased a system that is similar to the ones used in these references. It differs from the first in that it is not capable of receiving the military p-code signals. It is capable of differential carrier-phase calculations and should demonstrate good performance in similar applications on general aviation aircraft.

CHAPTER V

TEST ITEM DESCRIPTION

The aircraft being used for this testing is a Gulfstream American AA-5B Tiger serial number 001. The Tiger is a low-wing, single engine, four-place general aviation aircraft. This aircraft is a pre-production model that uses a Gulfstream American Cheetah airframe combined with the Avco-Lycoming O-360-A4K engine upgrade that is used in production models of the Tiger. The O-360-A4K is a normally aspirated, direct-drive, horizontally opposed, carbureted, four cylinder 360 cubic inch engine. It produces 180 HP at 2700 RPM.¹³ Although the object of the testing is to obtain takeoff and landing data on this aircraft, the aircraft itself is not the test item. Raspet Flight Research Laboratory's new Differential Global Positioning System (DGPS) is the actual test item. The object of this testing is to prove that this new system can work reliably as a source of time-space position information (TSPI) in flight test. Specifically, it is to determine the system's usefulness in providing useful TSPI in the high acceleration environment of takeoff and landing tests on a typical general aviation aircraft.

The NavSymm XR-5M12 GPS Receiver

The NavSymm XR-5M12 receiver is a state-of-the-art L1 C/A GPS receiver manufactured by Navstar systems Ltd. in the United Kingdom. It contains two proprietary 6-channel digital tracking receivers running in parallel. This gives the receiver 12 parallel tracking channels and enables it to have continuous carrier lock on all satellites in view (usually no more than 10 at any time) simultaneously. This equipment is sealed in a MIL-STD-810 IP67 die-cast aluminum box. The receiver can work either as a mobile receiver or as a differential base

station. RFRL's receivers contain firmware version 3.7. Interface with the unit is accomplished via the NavSymm Control-Display Unit Software (CDU) operating on an MS-DOS (or emulator) equipped personal computer (PC). Communication takes place through a standard 9-pin RS-232 port. The receiver publishes raw time-tag, pseudo-range and carrier phase information internally at 4Hz and may be accessed using the accompanying software. This data can then be used in post-processing.

The receiver is designed for DGPS operations. However, the manufacturer claims highly accurate stand-alone measurements as well. The manufacturer has classified the internal measurement noise. They claim an internal measurement resolution of 10-20 cm in pseudo-range and .7mm in carrier phase. The low pseudo-range noise is achieved by using a phase lock loop where the phase rate is fed back into the code tracking loop.

GPS Hardware Configuration For Flight Test

The base station receiver is an XR-5M12 receiver, serial number 67655. The receiver antenna is placed on a surveyed position atop the RFRL tower. It passes 1Hz data via the COM1 serial port of a GATEWAY 2000 Solo Colorbook Pentium-90 laptop computer. Initialization of the receiver is accomplished using xr5m.exe. The program nav1237.exe records the raw timetag, pseudorange, and carrier phase information.

The mobile receiver aboard the test aircraft is an XR-5M12 receiver, serial number 65644. The receiver antenna is located on the spine of the aircraft. The receiver passes 1Hz raw GPS data to another Gateway 2000 Colorbook 486-DX100 laptop computer, which records the data via nav1237.exe. The mobile receiver is initialized after engine start at a surveyed site and allowed to operate in static mode for several minutes prior to taxiing. The data collected by the receiver/PC combination is then processed post-flight.

GPS Data Post-Processor

Post processing of the collected GPS data is accomplished using software provided by Premier GPS, Inc. of Ontario, Canada. The primary data processing engine of the system is GPS_PROC.exe. It operates in conjunction with a pre- and post-processor called GRAFNAV.exe. This program allows you to read in and display the pre-processed data, define the processing options, manipulate the data, create various output files and display information to the screen.

Although several methods of kinematic processing are available in the software, kinematic positioning with initialization is best suited to this application. This is a carrier phase technique, with the carrier phase ambiguities being set by initializing the mobile receiver at a known point. The known point is computed using a quick static solution. Premier GPS claims accuracies of 2-5 cm + 2-3 ppm are maintained while continuous lock is kept on at least 4 satellites.¹⁰

The data processing algorithms consist of a Kalman filter to process the double differenced (DD) carrier phase, pseudorange, and carrier phase based on delta-range or Doppler measurements. The state vector of unknowns consists of the mobile receiver's position and velocity vectors and the DD carrier phase ambiguities.¹⁰ In this architecture, the carrier phase and pseudorange measurements tend to only contribute to the position and ambiguity states, while the delta-range or Doppler measurements tend to only contribute to the velocity states. As processing continues, the DD ambiguity standard deviations reduce. The filter pays more attention to the range information from the combination of the DD ambiguity estimate and the carrier phase measurements.

Once the processing is complete, the processing and position history are saved and the position history is plotted on the screen. The position history can also be saved in any datum desired using any unit system desired.

Manufacturer's Kinematic Tests

Navstar Systems Ltd. of the UK released the data from the system verification tests they performed at the Buntingthorpe test circuit.¹⁰ Using the same system configuration shown above, they mounted the mobile receiver in a standard sedan and drove the circuit at 120 miles per hour (mph). They did not have access to centimeter accuracy truth data for the circuit. Their solution was to look at the repeatability of the height profile as the car ran the track. The spread of the height results was 3 cm. Since height is the worst axis of measurement, they inferred that the horizontal results would be even better, to within 1 cm. The manufacturer did not however speak to the velocity accuracies or the position accuracies during accelerated maneuvers. This information is integral to takeoff and landing tests and remains an unknown.

RFRL's Verification Tests

In order to establish a baseline and confirm the manufacturer's claims of system accuracy, several tests were performed. The first involved a static GPS survey of a highly accurate B order surveyed site. The tests confirmed a 20 cm horizontal accuracy and a 30 cm vertical accuracy. The system was then placed on a moving vehicle. Velocity accuracy was confirmed to within 1 mph between 20 mph and 80 mph by radar (the measurement precision limit of the radar).

CHAPTER VI

REQUIRED MEASURANDS, APPARATUS, AND CALIBRATION

In order to determine the effectiveness of the GPS sensor, we must have a standard by which to compare. Once the standard is found we must determine what the required measurements are and how to obtain those measurements. In the case of takeoffs and landings, the air phase and the ground phase each provide unique problems in measuring the ground distance covered. As a result different techniques will be used for each.

Measuring The Ground Phase

Measuring the ground phase is as simple as measuring the distance between two points. For takeoffs the distance between the brake release point and the liftoff point is measured. For landings the distance between the touchdown point and the full stop point is measured. As a result, there are only four measurands required: brake release, liftoff, touchdown, and full stop.

Chapter III discusses several methods which can be utilized for these measurements. The aircraft used does not have an accelerometer package, and RFRL does not operate any radar or laser trackers. The only methods remaining that are available are the simple and relatively inaccurate. The brake release point is assigned prior to flight and the full stop point can be easily and accurately marked on the runway by an observer. This leaves the troublesome task of measuring the liftoff and touchdown points. The first method places people along the side of the runway to "spot" liftoff and touchdown. Assuming that the aircraft touches

down on the centerline and that both wheels touchdown at the same time (requires a no-wind condition), two "spotters" can be used to mark the touchdown with relative accuracy (probably within 15 ft of the actual point). The second measurement technique is the video-theodolite adapted from the USAF FTE handbook. This method uses a high resolution video camera and equally spaced markers along the runway. The runway markers provide the azimuth scale during data reduction. The geometry used is shown below. A Sony Hi-8mm video camera was placed 85 feet from the center marker. The markers were placed 80 feet from the runway centerline. The primary markers were placed 50 feet apart and the secondary markers were placed 16.67 feet apart. The resulting geometry is used to find the touchdown or liftoff points from the video data. This provides accuracy to within 10 ft.

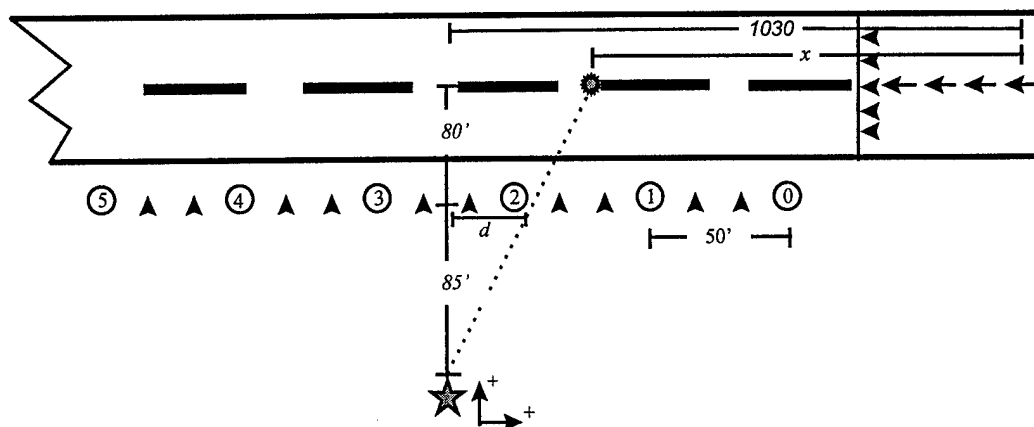


Figure 6.1: Video-Theodolite Geometry at Starkville-Bryan Field

Measuring The Air Phase

The beginning of the air phase is defined as liftoff or passing 50 feet AGL for takeoffs or landings respectively. The end of the air phase is defined as passing 50 feet AGL or touchdown for takeoffs or landings respectively. The video theodolite used in the ground phase is not capable of determining elevation, so another method must be found. Chapter III describes that an on-board air data acquisition system can be used for determining the length of the air phase.

The altitude, altitude rate, and airspeed information are converted to ground speed and then integrated to yield the air distance. RFRL has developed a compact 64 channel data acquisition system with a 12-BIT 0-10 volts analog to digital (A/D) board for general aviation aircraft. This system can be used in conjunction with the standard Rosemont and Sensym pressure transducers available for use at the lab.

A 5 foot pitot-static boom with a flying probe is installed on the wingtip of the Tiger. The boom moves the pressure ports outside of the aircraft pressure field and the flying head keeps the pitot probe aligned with the relative wind. These are connected via standard Tygon tubing to altitude and airspeed transducers in the wingtip. The transducers put out signals proportional to the altitude, the altitude rate, and the airspeed of the aircraft.

A 120-ohm strain gauge is mounted to the bottom of the right main landing gear at a gross weight of 2200 lbs. This gauge will be used as an event marker to determine weight on/off wheels. This is one of two indicators of liftoff and touchdown. Also being measured are engine RPM, engine manifold pressure, and a pilot event switch. The manifold pressure is obtained through a 't' fitting on the emergency vacuum system. The pressure is transferred to a SenSym pressure transducer through tygon tubing. The PC is capable of sample rates ranging from 1 to 1000 Hz. The system is operating at 50 Hz during test points. The PC clock was synchronized to GPS time prior to each flight and re-verified postflight.

The altitude transducer signal is passed through a 10 times amplifier in order to increase the altitude resolution. The vertical velocity signal is given a 5-volt offset so that both positive and negative voltages can be recorded. All signals are passed through a 20 Hz low-pass filter before arriving at the (A/D) board and finally recorded on a desktop PC in binary format as raw voltage output. The filter eliminates any high frequency noise from the data and therefore eliminates the resulting aliasing frequency.

Sensor Calibration

Quality transducers and accurate calibrations are the key to obtaining good air phase data. All data instrumentation should be calibrated in conditions that simulate those of the test environment. All of the following sensors were calibrated on the aircraft and using hangar power through the aircraft bus.

Both the altitude and airspeed pressure transducers were calibrated throughout their useful range using a Mensor pressure regulator. This regulator can regulate pressures from 0 to 15 psi at .001 psi intervals. A piece of Tygon tubing connects the Mensor to the static ports on the flight test boom. The total pressure port is left open to the atmosphere.

The airspeed transducer is a Rosemount 1221D1B1 serial number 53. This transducer measures the differential pressure between the static and the total pressure sources. It has an effective range of 30 to 130 knots at approximately 50 mv per knot. To calibrate this transducer, the delta pressure corresponding to a given airspeed is found and subtracted from the current atmospheric reading. This pressure is dialed into the Mensor and the voltage output is recorded. The airspeed transducer is calibrated in this manner from 30 to 120 knots in 5 knot intervals. This was done by starting at 30 knots and increasing to 120 knots then continuing back down to 30 knots. The calibration curve was obtained by averaging these values then applying a fourth order polynomial fit. The resulting fit was

$$V_e = -.051v^4 + 1.189v^3 - 9.011v^2 + 47.515v - 30.864 \quad (6.1)$$

where V_e and v are the equivalent airspeed and the transducer voltage output respectively.

Figure 6.2 shows the resulting data and curve fit.

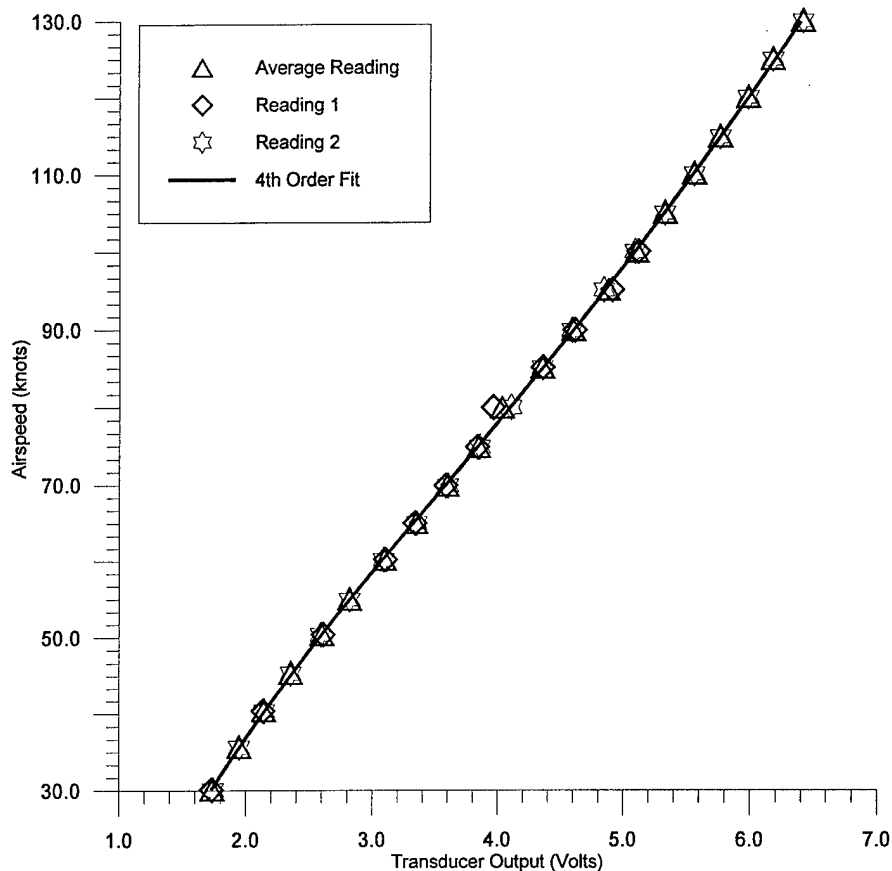


Figure 6.2: Rosemount Airspeed Transducer Calibration
Model: 1221D1B1 S/N: 53

The altitude transducer is a Rosemount 1241A4BCD serial number 345. It has a range of 0 to 30,000 feet at .25 millivolts per foot. Since the signal is amplified, the output seen at the data system does not match and is approximately 2.5 millivolts per foot. This transducer is calibrated for the altitude range of interest, specifically 0 to 1,000 feet in 100 foot increments. The calibration is accomplished by dialing the standard atmospheric pressure for a given altitude into the Mensor and the voltage output is recorded. A linear curve fit was applied to this data and is shown below:

$$h = 410.89v + .055 \quad (6.2)$$

Where h and v are the pressure altitude and the transducer voltage output respectively. Figure 6.3 shows the resulting calibration data and curve. The altitude transducer is also equipped with a vertical velocity signal at ± 50 mv per foot/sec. The manufacturers' calibration of this parameter is used and has not been independently verified.

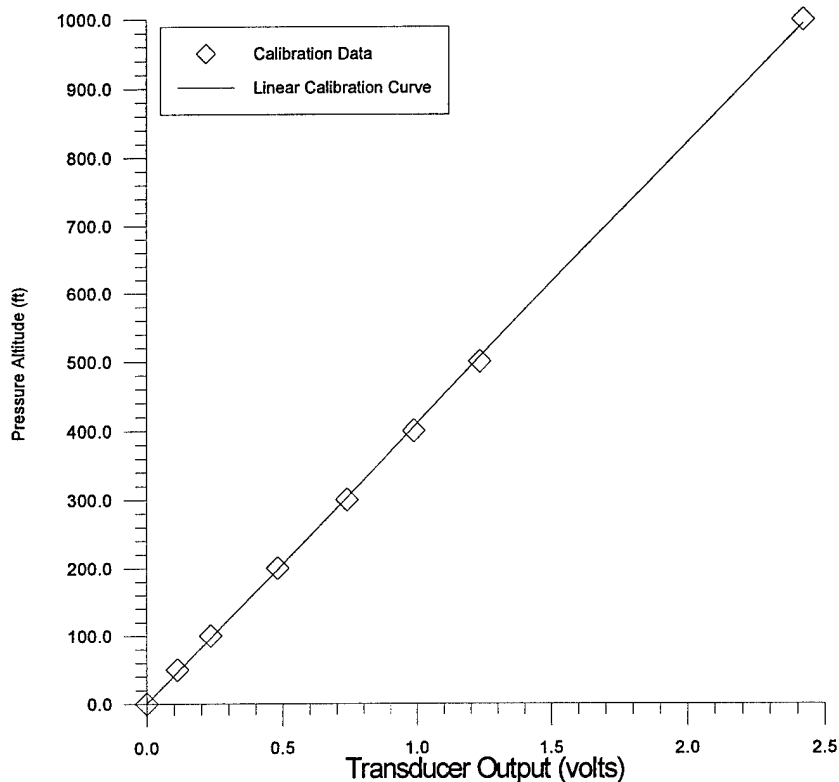


Figure 6.3: Rosemount Altitude Transducer Calibration
Model: 1241A4BCD S/N: 345

The SenSym pressure transducer was calibrated from 1.5 to 14.5 psi in 1psi increments. The Mensor was connected to the vacuum t fitting. The voltage out is recorded for each pressure. The engine RPM sensor is a digital counter and does not require calibration. Since the strain gage and the event markers are needed for raw output voltage only, they do not require calibration.

CHAPTER VII

TEST EXECUTION

Takeoff and landing tests are susceptible to the environment and to pilot technique. It is therefore important to standardize the piloting techniques used, the preflight actions, the weather minimums, as well as the test team actions during each test point. If this is done well, the standard deviation will be minimized.

Preflight Actions

Prior to each flight the data system is spot-checked to verify proper operation and calibration of the data acquisition system. First the Mensor must be turned on for at least an hour prior to use. It can be turned on while other preflight actions are taking place. The weather is checked against the minimums. The primary minimums for these tests are: a) no visible moisture b) visual flight rule minimums c) winds maximum of 5 knots with a maximum gust factor of 5 knots. After the weather is verified the on-board PC clock is synchronized with current GPS time. Once the Mensor has been on for an hour, the remaining checks are completed.

Atmospheric pressure is obtained by measuring it with the Mensor. The output voltage from the manifold pressure transducer is checked to verify that it is displaying atmospheric pressure. The altitude transducer is spot-checked at pressures correlating to 100 feet, 500 feet, and 1000 feet. The airspeed transducer is spot checked at pressures correlating to 30 knots, 60 knots, and 90 knots. Finally the voltage output from the event marker and the weight on/off wheels sensor is checked. The runway markers are set up prior to the briefing.

Test Team Actions

Finally, when all preflight actions are complete, the test team should be briefed on their actions. Seven people are required to run this test. The pilot and a flight test engineer are required to fly the aircraft, to run the data acquisition system, and to run the GPS. Two "spotters", a camera operator, a full stop "marker", and a test conductor are required. The spotters stand 100 feet apart on the far side of the runway and mark the liftoff and touchdown points of the main landing gear (MLG) with paint on the runway. The camera operator films every takeoff and landing from brake release to liftoff and from touchdown to full stop. The marker annotates the full stop position of the MLG on the runway with paint. The marker also gives a countdown to full stop on the to time tag the data sources. The test conductor gives a countdown to brake release for the pilot and monitors air traffic in the area.

The GPS system and the data acquisition system are initialized at the point marked "B" on the RFRL Annex taxiway. This allows the GPS to start from a known position. The GPS datalogger is started in static mode. This position is held and static data is collected for 200 to 400 seconds. The data acquisition system is also run through all modes to verify its operation prior to flight. Once this action is complete, the GPS datalogger is switched to kinematic mode and the aircrew taxis into position for the first test point.

Standardizing Takeoff Procedures

The pilot technique must be standardized for each takeoff performed. Chapter III mentions several parameters that are important to standardize. The pilot must line up the MLG on the first arrow in the displaced threshold. This position ensures that liftoff will occur within the range of the runway markers. Five degrees of flaps are selected for takeoff. The throttle is to be set full open and the rpm stabilized prior to brake release. The test conductor then gives a countdown, "3 . . . 2 . . . 1 . . . release." Coincident with the word "release" the brakes are released. The controls are held to keep the aircraft in a 3 point position until 57 knots. The aircraft is then

rotated to immediately lift off the runway. The pilot then maintains 65 knots until 50' AGL is passed.

Brake Cooling

The pilot will then fly a long and fast downwind leg to ensure that the brakes have fully cooled prior to the next landing. This is important since repeated takeoffs and landings will build up a lot of brake energy, and therefore heat, in the brakes if they are not properly cooled on downwind. The consequences of not keeping the brakes cool can be severe. Anything from blown tires to brake meltdown or brake fires can result.

Standardizing Landing Procedures

Full flaps are selected on long final. The pilot then maintains an airspeed of 65 knots and power as required to maintain a 3° glideslope. The aimpoint is adjusted as required by the pilot to touchdown within the azimuth marker range. The flare occurs at approximately 10 ft. The pilot ensures touchdown occurs within the desired range. For this test, the location of touchdown is more important than the rotation rate at flare or the touchdown airspeed. These are adjusted as required by the pilot to land in the required area. After touchdown moderate braking is used. The pilot adds slightly more brake pressure as the airspeed decreases and more weight is put on the MLG.

Postflight Procedures

Dekker and Lean recommend that at least 6 takeoffs and landings be conducted for statistical significance. After the flight is complete, the aircraft must return to the initialization point on the RFRL Annex taxiway. The GPS datalogger collects a few more seconds of static data on the surveyed point as the data acquisition system is shut down. The GPS datalogger is then shut down and the GPS system turned off. Testing is complete at this point and the aircrew taxis back to the ramp.

CHAPTER VIII

DATA REDUCTION

In this experiment, there is a large amount of data reduction to be done. First the truth data sources must be reduced. This includes reducing the video theodolite data for the ground phase and reducing the air data for the air phase of each takeoff and landing. Once this is complete, the experimental GPS data must be reduced for both the ground and the air phase. The data reduction methods used on the GPS data are an integral part of the project's success.

Spotter and Video Theodolite Data Reduction Methods

During each takeoff test point, spotters mark the observed liftoff point of the aircraft with paint on the centerline. During each landing the spotters mark the observed touchdown point of the aircraft and a marker annotates the full stop point of the aircraft. Using a precision measuring wheel to measure these distances from the runway origin easily reduces this data. The runway origin is defined as the brake release point abeam the first arrowhead in the displaced threshold. All of these measurements are taken immediately after each flight.

The video data was a little more complicated to reduce. The calibrated marker method from chapter III is used to find the liftoff and touchdown points. Equation 8.1 is the applicable equation with the specific known distances entered (the actual geometry is shown in Figure 6.1).

$$x = 1030 - 2.0625 * d \quad (8.1)$$

It can be seen that the quantity d , the distance from the camera line to the apparent marker position is needed. A frame by frame analysis yields the liftoff and touchdown points of each event in relation to the runway azimuth markers. This event occurs at some ratio of the

distance between markers as shown on the screen. This ratio is multiplied by the known distance between the markers to find d . Once d is known, Equation 8.1 solves for the touchdown or liftoff point.

Air Data System Data Reduction Method

The air data system is the primary truth source for the air phase distance calculations. Ward states that the airspeed data can be used to produce a smooth velocity history after rigorous data reduction. Since the air data is derived from a 5 foot flight test boom, the position error correction is assumed to be negligible. The transducer calibration curves include any instrument error and is therefore incorporated into the voltage to engineering unit (EU) conversion. It can be assumed that the EU conversion output is equivalent airspeed, V_e . The remaining processes required to obtain the air phase distance are data smoothing, converting V_e to ground speed (V_g), and integrating velocity from liftoff to 50 feet above the runway origin.

There are small data fluctuations in the data obtained by the RFRL data acquisition system due to the A/D card resolution. In order to eliminate the fluctuations, a moving window averaging filter is used. The following equation shows the filter equation used.

$$x_i = \frac{x_{i-4} + x_{i-3} + x_{i-2} + x_{i-1} + x_i + x_{i+1} + x_{i+2} + x_{i+3} + x_{i+4} + x_{i+5}}{10} \quad (8.2)$$

The data was taken at 50 Hz, therefore this corresponds to a window width of .2 seconds.

Equation 8.2 was used to filter all the air data information; altitude, vertical velocity, and airspeed.

Assuming no-wind conditions exist, the air data is then converted to ground speed, V_g .

This is accomplished by using the vertical velocity, \dot{h} , and the equivalent airspeed in the following transformation. V_g is then integrated to yield the air distance.

$$V_g = V_e \cos(\gamma) \quad (8.3)$$

where

$$\gamma = \sin^{-1}\left(\frac{\dot{h}}{V_e}\right) \quad (8.4)$$

The liftoff point is identified by a sudden increase in vertical velocity. The touchdown point is identified by a sudden decrease in descent rate. These markers are used because they do not require good time synchronization between the air data and GPS sources. Once these events are identified a simple Euler integrator is used from the start of the event, liftoff or 50 feet, to the end of the event, 50 feet or touchdown. Equation 8.5 is the integrator used.

$$S_a = \int_{t_o}^f V_g dt = .02 \sum_{t_o}^f V_g \quad (8.5)$$

A spreadsheet is used for these calculations.

GPS Data Reduction

The GPS data logger programs store raw receiver information in a binary format file. This data must be converted to standard velocity units and Universal Trans Mercator (UTM) coordinates. This is accomplished with the software provided by Premier GPS, Inc. of Ontario, Canada. There are two programs provided for post-processing. The first is GPS_PROC.exe which is the actual data processing engine. The other is GRAFNAV.exe, which is a graphical pre- and post-processor for GPS_PROC.exe. Without going into the details of program operation, the .out and .utm files are output for velocity and position information in data reduction. The .out file should then be manually disassembled into data sets that only include the takeoff and landing events.

A simple program was written that loads the data files and then uses two different algorithms to determine the ground and air phase distances. The first method involves integrating the GPS velocity to get distances. The second method uses the position information to directly calculate distances.

Takeoffs will be considered first. The algorithm searches for the first indication of increasing ground speed. The tolerance used is .3 ft/sec. Brake release is assumed to occur at

the previous epoch. The UTM coordinates and altitude of the brake release are recorded for future use. Trapezoidal integration of the GPS ground speed, V_g , is used to calculate the distance from brake release at each second. Equation 8.6 is used.

$$S_{G_i} = \int_{t_0}^{t_i} V_G dt = S_{G_{i-1}} + \left(\frac{V_{G_{i-1}} + V_{G_i}}{2} \right) (t_i - t_{i-1}) \quad (8.6)$$

The numerical integration continues until the GPS vertical velocity rises above a user-defined tolerance. This is considered to be the liftoff point and the current value of S_G is used as the final solution. The UTM coordinates of the liftoff point are recorded. With the brake release coordinates and the liftoff coordinates available, Equation 8.7 is used as a second solution to S_G .

$$S_G = \sqrt{(N_{BR} - N_{LO})^2 + (E_{BR} - E_{LO})^2} \quad (8.7)$$

where N_{BR} , N_{LO} , E_{BR} , and E_{LO} are the northing and easting coordinates at brake release and liftoff respectively.

The algorithm continues, now calculating the air phase distance. Trapezoidal integration is used to calculate the distance from liftoff at each second according to Equation 8.8.

$$S_{A_i} = \int_{t_0}^{t_i} V_G dt = S_{A_{i-1}} + \left(\frac{V_{G_{i-1}} + V_{G_i}}{2} \right) (t_i - t_{i-1}) \quad (8.8)$$

The numerical integration continues until the height above brake release is greater than 50 feet. The extra ground distance covered between the last epoch and 50 feet, $S_{A_{extra}}$, is then linearly interpolated according to

$$S_{A_{extra}} = V_G \Delta t_{extra} = \frac{(h_{50} - h_i)(V_{G_{i-1}} + V_{G_{i-2}})}{2\dot{h}_i} \quad (8.9)$$

where Δt_{extra} is the time required to climb from the last known altitude to 50 feet above brake release based on the current vertical velocity. This value is added to the final value of S_A to yield

the total air phase distance. The last known coordinates and $S_{A_{extra}}$ are used for the alternate calculation of S_A according to Equation 8.10.

$$S_A = \sqrt{(N_{LO} - N_i)^2 + (E_{LO} - E_i)^2} + S_{A_{extra}} \quad (8.10)$$

Finally, the total takeoff distance for each method is calculated with Equation 8.11.

$$S = S_G + S_A \quad (8.11)$$

This algorithm can be used for landings with minimal modification. A landing is essentially a takeoff in reverse. By searching for the full-stop and using backward integration, this algorithm can be used for landing distance calculations. This is implemented using a direction flag in the program. If positive, forward integration is used. Otherwise landing distance is being calculated and backward integration is used.

Reduction to Standard Day Conditions

Takeoff and landing flight test data is usually reduced to standard day conditions. The equations to accomplish this are fairly straight forward. However, this test has been designed to evaluate the position, velocity, and distance measurements directly. Standard day reduction goes beyond the scope of the testing and will not be accomplished.

Algorithm Modifications During GPS System Verification Tests

Prior to flying any test points, the GPS system was installed and its operation verified. There were several verification test flights conducted. The data collected on these flights is fairly good. These flights necessarily included takeoffs and landings. The data from these landings provided algorithm verification. As a result, two changes were made to the algorithm.

The first problem area is the GPS vertical velocity. It consistently begins to increase before any change in altitude is apparent as shown by figure 8.1. The GPS vertical velocity even overshoots the actual by a substantial amount. Figure 8.1 shows GPS vertical speed and the first derivative of altitude.

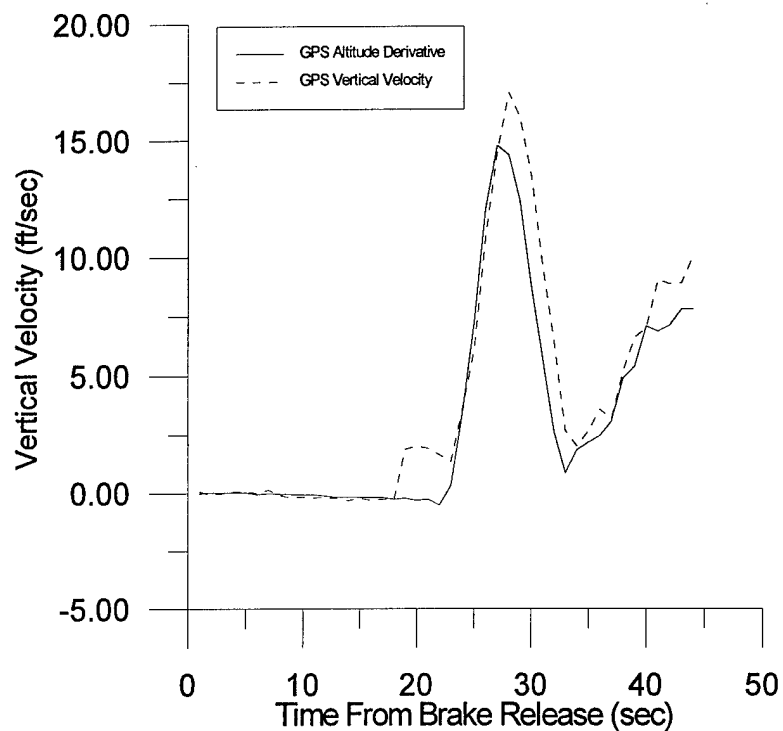


Figure 8.1: Vertical Speed Comparison from Takeoff No. 10

Due to this problem, it was decided to use the altitude derivative for vertical speed in the algorithm. The following equation is now implemented in the algorithm.

$$\dot{h} = \frac{dh}{dt} = \frac{h_i - h_{i-1}}{t_i - t_{i-1}} \quad (8.12)$$

CHAPTER IX

PRESENTATION OF RESULTS

Two flights were conducted over a two week period. The first data flight, GPS-04, was conducted on September 8, 1997. Six takeoffs and six landings were conducted. The weather on this date was marginal for winds. The winds were approximately from 200° at 5 knots with a 5 knot gust factor. The second data flight, GPS-05, was conducted on September 30, 1997. There was no significant weather on this date. Eight test points were conducted. However, the first two points were flown with a different technique and were discarded.

In this discussion of the results, takeoffs and landings are discussed separately. These are further broken down into the respective ground and air phases. The video theodolite data is considered to be the truth source for the ground phase data. Although the video data yields approximately the same accuracy as the observation data, it can be repeatedly analyzed frame by frame. This lends greater confidence to the measurements taken with the video theodolite method. It usually correlates to within ten feet of the observation data on most runs. On the few that the correlation is bad, the observers were found to be in error. This is to be expected, since the observers had one chance to take a measurement traveling at nearly 100 feet per second. Since there was no elevation scale for the video theodolite data, the air data calculations are considered to be the truth source for the air phase data.

According to Ward, full position velocity and acceleration profiles of takeoffs can be a useful analysis tool. Air data is not particularly useful for this application for two reasons. First, it takes rigorous post-processing to convert it to an inertial reference system. Second, most

airspeed transducers are not reliable below 30 to 40 knots. GPS data is, by definition, presented in an earth-fixed inertial reference system. GPS velocity is reliable down to .5 knots. This makes it an ideal tool for producing these profiles.

GPS Variable Position and Velocity Lag

It was originally intended to determine the liftoff and touchdown points with the weight-on/off-wheels (WOW) signal available from the on-board data acquisition system (DAS). Prior to every flight the DAS time was synchronized with current GPS time. Unfortunately, postflight analysis reveals a GPS data time lag. The DAS weight off wheels WOW signal occurs as much 5 seconds before the GPS data shows any increase in vertical speed. Additionally, using the WOW signal to calculate ground roll yields measurements that are hundreds of feet short of the actual. The next step is to compare the time at which the DAS and the GPS vertical speeds start increasing. Again the GPS vertical speed increase significantly lags that of the DAS. This critical time lag is easily apparent in Figure 9.1 which shows the DAS WOW history, DAS vertical speed history, and the GPS vertical speed history for takeoff number 13.

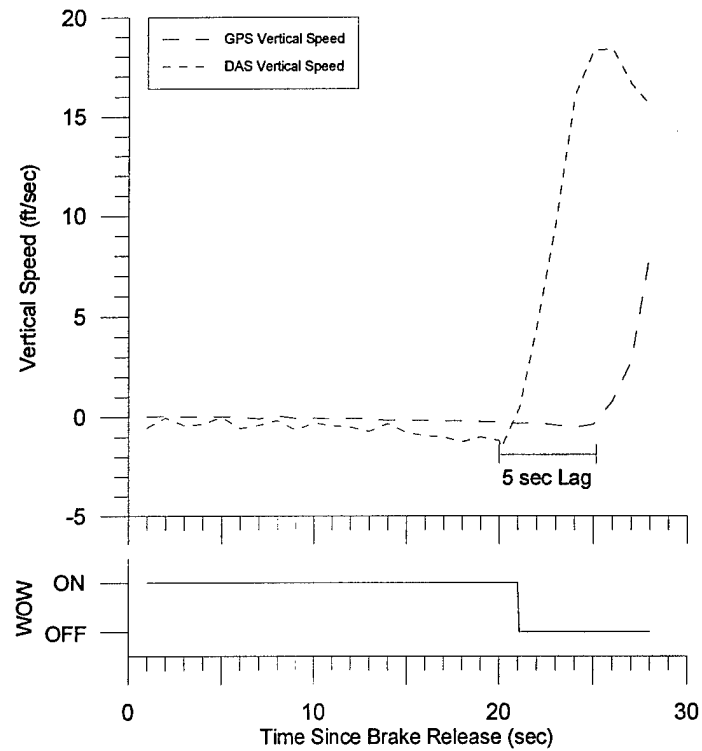


Figure 9.1: GPS and DAS Vertical Speed Profiles for Takeoff No. 7

Further analysis reveals that the lag decreases with flight time. Figure 9.2 shows this bias as a function of time for flight GPS-05. The time error shown is found by comparing the vertical velocity changes shown on the GPS data record and the air data record. The time dependency of this lag is the key to finding its source.

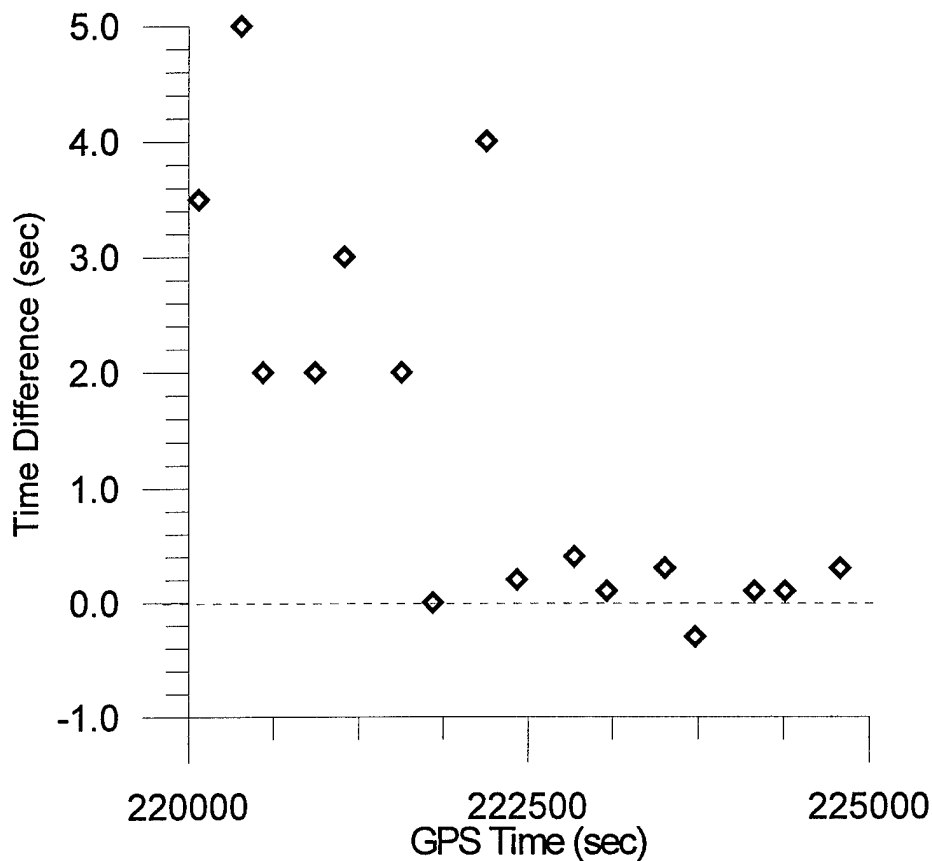


Figure 9.2: Position Time Lag History for Flight GPS-05

This time error is probably a function of the quality of the GPS carrier phase ambiguity solution. The filter initially pays very little attention to the double differenced (DD) carrier phase ambiguity information contained in the state matrix. However, as time increases and the carrier phase ambiguity decreases, the filter incorporates the DD carrier phase ambiguity information into the position and velocity state solutions. The introduction of this information could be the reason for the decrease in the lag over time. The filter algorithm is proprietary, and information on its mechanics is not available at the time of this writing.¹⁴

There remains a residual time lag that is during the final 2500 seconds of the flight. This may be due to the filtering solution or it may have another source. The method of synchronizing the DAS by setting the on board computer clock to GPS time is not perfectly accurate. Due to

the human element involved, its probably only accurate to .1-.3 seconds. This approximately corresponds to the residual bias shown in the last 2500 seconds of the flight. The residual time lag allows neither good DAS-GPS synchronization nor the use of the DAS WOW signal in the GPS calculations. The change in GPS vertical velocity is the only available method of determining the liftoff point from the GPS data.

This was a simple matter for takeoffs. The GPS takeoff calculations can be modified to interpolate the liftoff parameters from the vertical velocity data. It can be seen in the data that on liftoff the vertical goes from negative to positive. This is due to the negative runway slope at Starkville-Bryan field. This is advantageous because a zero vertical speed point can be found using the second-order LaGrange interpolating polynomial shown in equation 8.13.

$$f_2(x) = \frac{(x-x_1)(x-x_2)}{(x_0-x_1)(x_0-x_2)} f(x_0) + \frac{(x-x_0)(x-x_2)}{(x_1-x_0)(x_1-x_2)} f(x_1) + \frac{(x-x_0)(x-x_1)}{(x_2-x_0)(x_2-x_1)} f(x_2) \quad (9.1)$$

In the case of solving for vertical velocity, $f_2(x)$ is vertical velocity at the interpolated time step (i.e. at the $i-2$ time step), $f(x_0)$, $f(x_1)$, and $f(x_2)$ are the values of vertical velocity at the i , $i-1$, and $i-2$ time steps respectively. The time step that yields a vertical speed of zero is found iteratively. This value of time is now considered to be the liftoff point. The ground speed, northing, and easting at liftoff are similarly calculated using Equation 8.13. This yields approximately 1 foot resolution for the ground roll calculations.

There is no clean distinction in the vertical velocity on landings from which to identify touchdown. As a result, there is no method used in this study which can positively identify the touchdown point. It is only possible to identify a range of values between which the actual landing air and ground distances lie. A half-second range was used for this purpose. Once the marked decrease in vertical velocity is found, Equation 9.1 is used to calculate the ground speed, northing, and easting at $t-.5$ sec.

Takeoff Ground Phase Results

The ground phase of the takeoff begins with brake-release and ends with liftoff. The liftoff point information is determined using the quadratic interpolation technique. Figure 9.3 shows the takeoff roll measurements for both flights. The video theodolite measurements are shown with the associated measurement accuracy error bars. Both the GPS velocity integration and the GPS position difference methods of calculating the ground roll are also shown. A glaring disparity in the ground roll measurements between the two flights is immediately apparent. They appear to be almost 400 feet longer on flight GPS-05. This is due to the differing wind conditions that existed on the two days.

There are several data trends that remain constant between the two flights. The GPS velocity integration technique gives results that are typically within the measurement accuracy bounds of the video-t data. There are only two points that are not within these bounds. Also, the GPS position difference method consistently over-predicts the takeoff roll and yields a solution that is greater than the velocity integration solution.

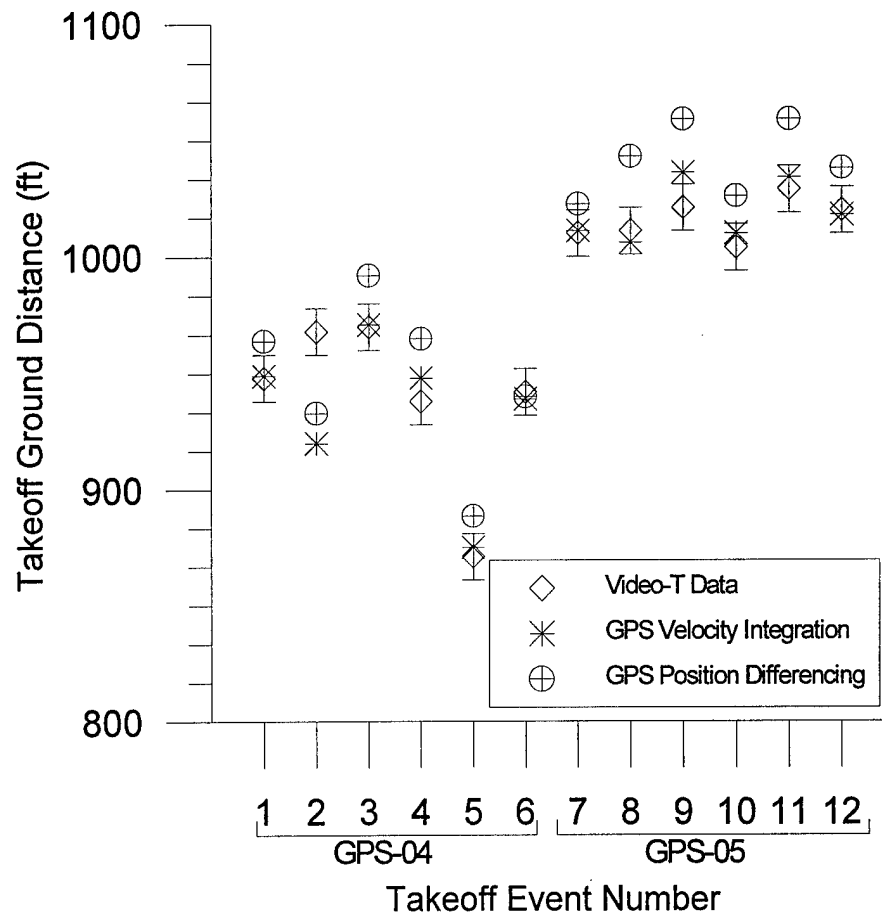


Figure 9.3: Takeoff Ground Phase Distance Measurements

Figure 9.4 shows the error associated with each measurement when the video theodolite data is used as the reference measurement. The error associated with GPS velocity integration is consistently within the 10 foot accuracy bounds of the video theodolite data. The maximum errors shown are -48 feet and +15 feet. The error associated with the GPS position differencing technique is consistently outside the 10 foot accuracy bounds of the video theodolite data. This error is consistently high, confirming that the method is substantially over-predicting the takeoff roll.

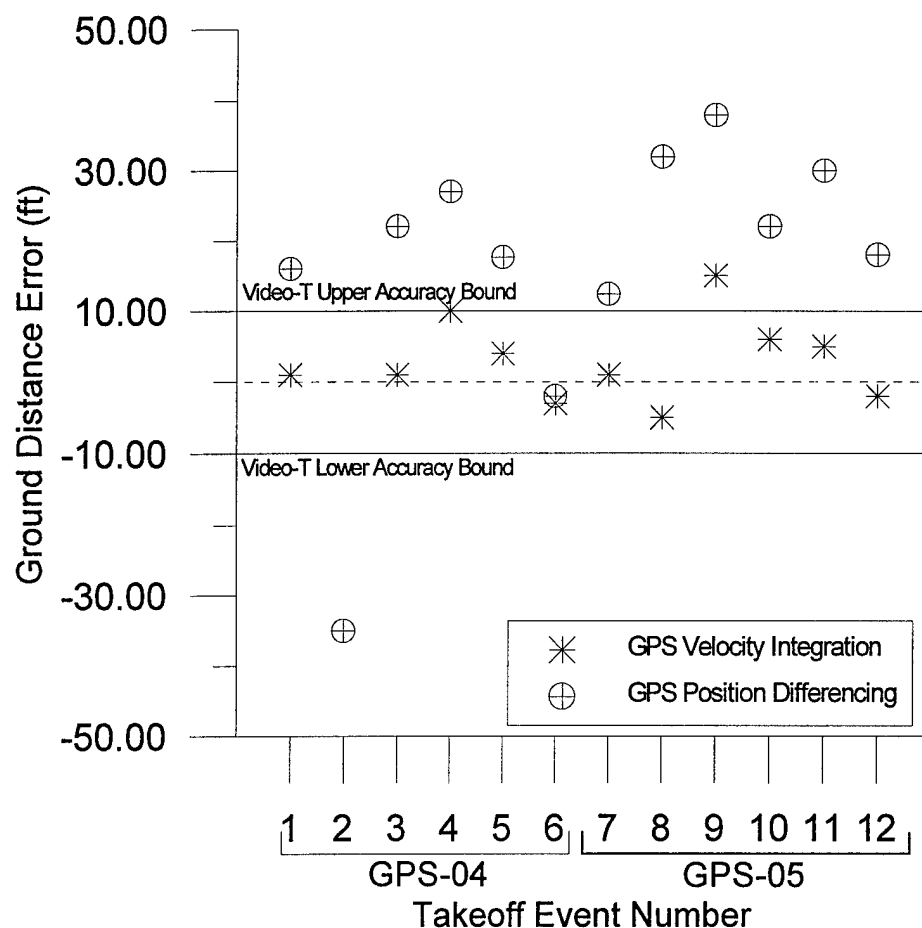


Figure 9.4: Error of Ground Roll Calculations

Further insight can be gained through a few simple statistical calculations. Table 9.1 shows the mean and standard deviation of the measurements and the measurement errors from flight GPS-04. This table shows that the average measured takeoff ground distance was approximately 934 feet with a standard deviation of 37.2 ft. This is a very large standard deviation and implies a large amount of scatter within the data. This scatter is due to the gusty wind conditions that were present during flight GPS-04. The velocity integration technique resulted in an average takeoff roll of 936 feet. This results in an overall error of 2.6 feet. These results demonstrate the apparent reliability of the GPS velocity integration technique. The GPS position technique resulted in an average takeoff roll of nearly 950 feet. The error associated

with this method is then 16.1 feet. This is well outside the video theodolite's 10 foot error band and demonstrates the unreliability of this method. It is also important to note the large standard deviations associated with these measurements. This implies a large amount of scatter in the data that is due the gusty winds present during flight GPS-04.

Table 9.1: Takeoff Ground Distance Calculation Statistics for Flight GPS-04

METHOD	MEAN (FT)	STANDARD DEVIATION (FT)	ERROR (FT)
Video	933.8	37.2	N/A
GPS Vel. Int.	936.4	36.3	2.6
GPS Pos. Dif.	949.9	38.9	16.1

Table 9.2 shows similar statistical results for mission GPS-05. This table shows that the average takeoff ground distance was approximately 1016 feet and that the error of the velocity integration method is 3.3 feet. The average error of the position difference method is 25 feet. Notice that the standard deviations associated with these measurements are substantially smaller due to the no-wind conditions existing during flight GPS-05.

Table 9.2: Takeoff Ground Distance Calculation Statistics for Flight GPS-05

METHOD	MEAN (FT)	STANDARD DEVIATION (FT)	ERROR (FT)
Video	1015.8	9.1	N/A
GPS Vel. Int.	1019.2	12.9	3.3
GPS Pos. Dif.	1041.2	15.7	25.4

Table 9.3 shows the error statistics of all the measurements from both flights. The average error of all the GPS velocity integration calculations is 3 feet with a standard deviation of 5.9 feet. These are exceptionally good results and imply that the GPS velocity integration method as implemented is a valid method. However, the average error associated with the position difference calculations is too high at 16.5. This implies that this method needs to be improved before it can be used to calculate the takeoff ground phase.

Table 9.3: Takeoff Ground Roll Calculation Error Statistics From All Flights

METHOD	MEAN ERROR (FT)	STANDARD DEVIATION (FT)
GPS Velocity Integration	3.0	5.9
GPS Position Differencing	16.5	19.2

The reason for the difference between the two solutions is apparent when considering the velocity information used in each solution. The GPS velocity integration technique uses the trapezoidal rule. In doing so, velocity is backward averaged. As a result, the velocity used in the integration technique is lower than the current GPS value. The difference between the time derivative of position and the GPS backward averaged velocity is shown in Figure 9.5 for takeoff number 19. Notice that the velocity difference is very small, averaging approximately 2.5 ft/sec. However, as this slight difference is integrated over time, the distance error increases considerably. The difference between the distance from brake release obtained through position differencing and velocity integration is also shown in Figure 9.5. As time increases, the difference increases because the small amount of excess velocity is getting integrated over time.

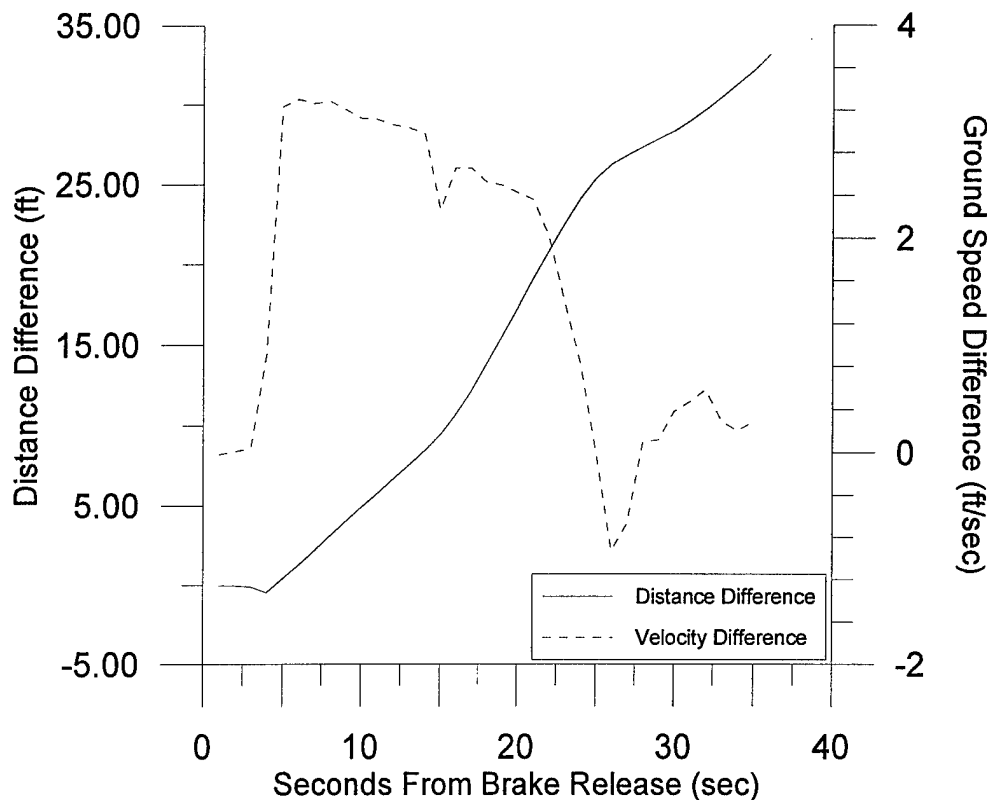


Figure 9.5: History of Position and Velocity Difference Between Integration and Position Techniques

Takeoff Air Phase Distance Results

The takeoff air phase begins at liftoff and ends at 50' AGL. Figure 9.6 shows the air phase distance measurement results. Due to air data wind susceptibility and the wind conditions during GPS-04, only the results from GPS-05 are shown. The reference measurement for the air phase distance calculations, obtained by integrating the air data, is shown. Also shown is the air distance calculated by integrating the GPS ground speed and differencing the GPS positions. There is a large amount of scatter in this data. Good correlation among the methods occurs in only two test points. It is also interesting to note that the position difference method yields results that are consistently higher than the velocity integration method.

This is happening for the same reasons it happens during the ground phase. The difference between the current velocity and the backward average velocity gets integrated over time.

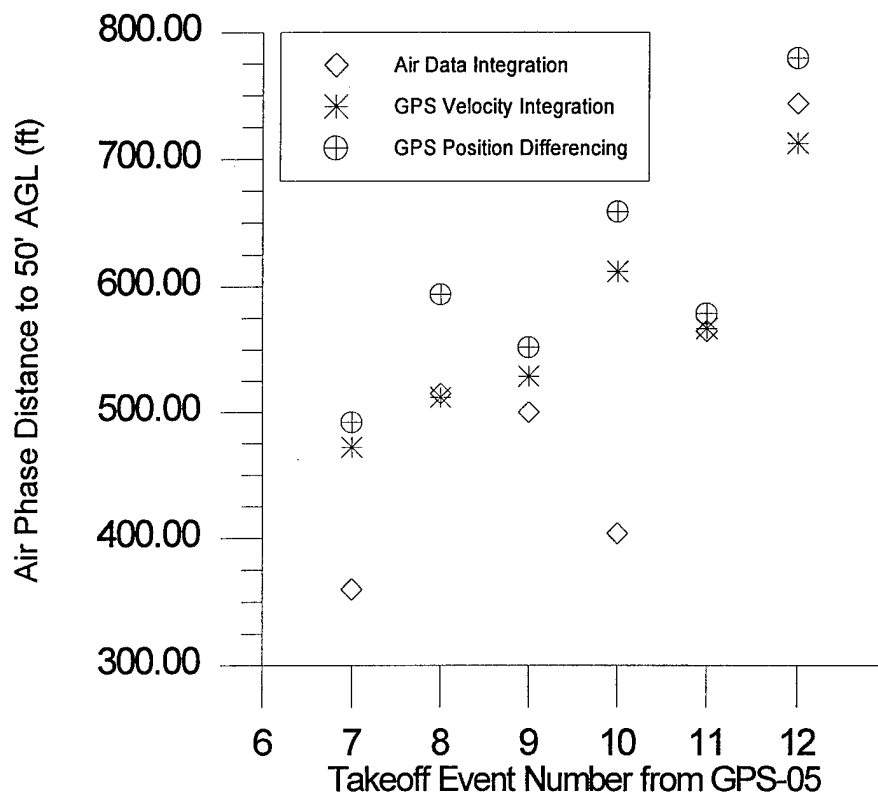


Figure 9.6: Air Distance Calculations for Flight GPS-05

The standard deviations for the GPS methods is only 90 feet. The standard deviation of the air data results is 135 feet. This is nearly 150% of the standard deviation of the other two methods. This raises questions about using the air data method as a truth source. As a result no reliable conclusions can be drawn about using the GPS methods to determine the air distance.

Takeoff Position and Velocity Profiles

With the takeoff distances known, it is useful to examine the position and velocity profiles of the takeoff. These plots allow for analyzing data trends and verifying calculations.

Figure 9.7 shows the horizontal distance and velocity profile for takeoff number 19. These

curves are very smooth. This is an expected result considering that the GPS data is filtered.

Notice that the ground roll distance of 1034 feet occurs as the weight comes off the wheels. The velocity continues to increase throughout the profile until liftoff where it remains constant for the climb out at 110 ft/sec.

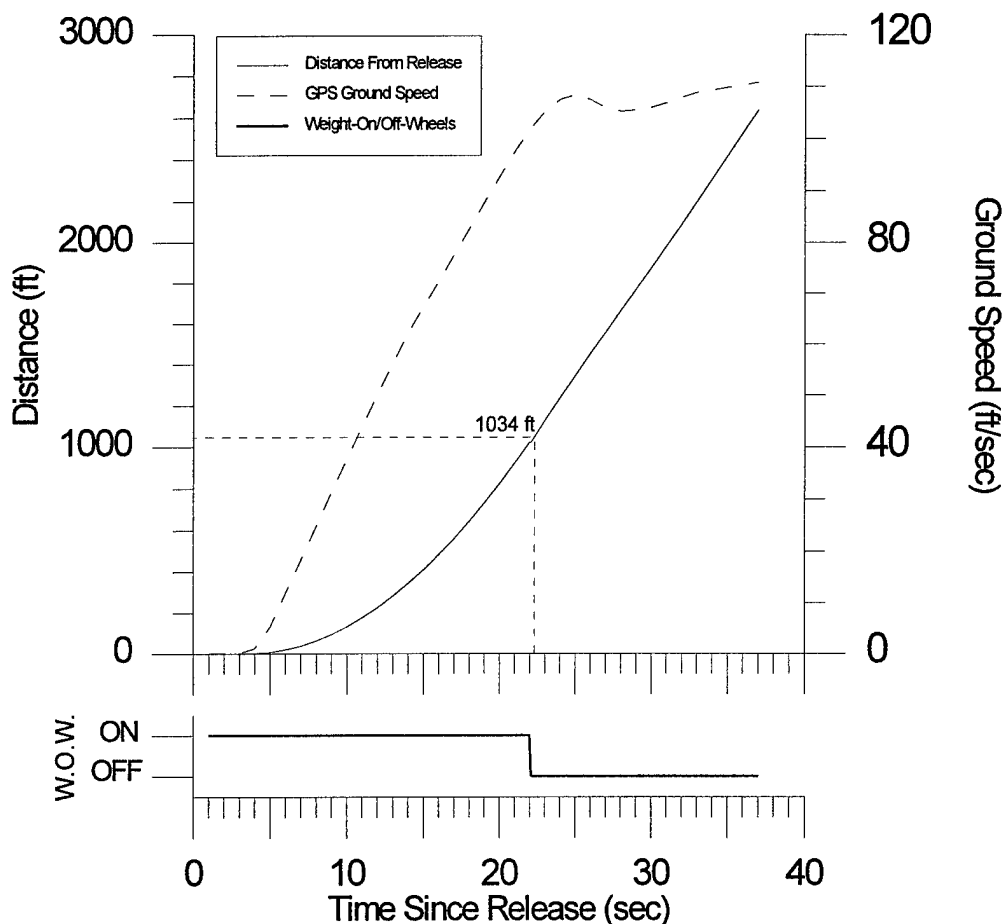


Figure 9.7: Position and Velocity Profiles for Takeoff No. 11

Figure 9.8 shows the altitude and vertical velocity profiles for takeoff number 19. It is interesting to note that the vertical velocity begins at a small negative value and the altitude is decreasing. This is due to the negative slope of runway 18 at Starkville-Bryan field. Notice that the altitude and the vertical velocity both are increasing as the weight comes off the wheels.

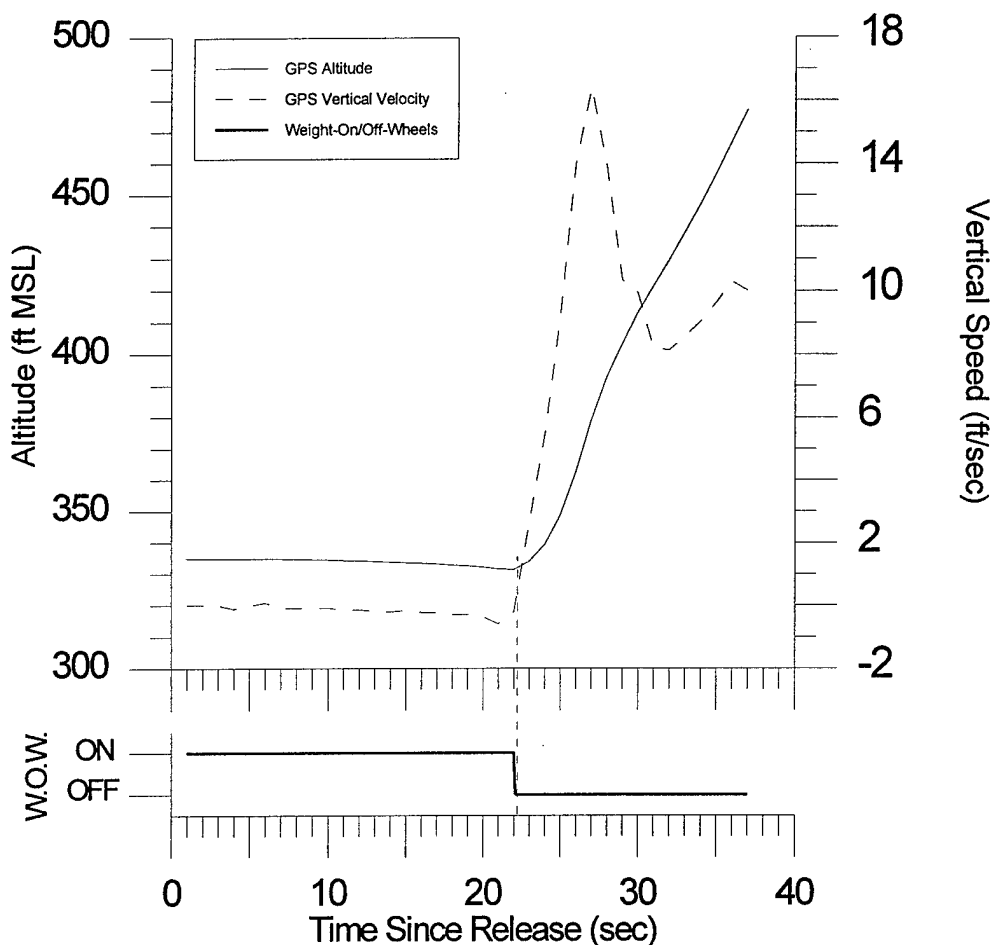


Figure 9.8: Altitude and Vertical Velocity Profiles for Takeoff No. 11

Landing Air Phase Distance Results

The air phase of the landing is the distance covered from passing 50' AGL to touchdown. As discussed earlier, a reliable method of determining the touchdown point was not found. As a result the GPS solutions are only good to a half second range, or approximately 50 feet. This results in a solution band marked by a high and low values for both the GPS velocity integration method and the GPS position difference method. The landing air phase distance results are shown in figure 9.9. The distance calculated by integrating the air data is shown and considered to be the reference measurement. Also shown are the half second air distance solution bands for each method. In all cases, both the GPS air phase distance calculation

methods are within 50 feet of the air data calculations. Both methods perform equally well, and have good correlation with the reference measurements. This is much better correlation than that found for takeoffs. The better correlation is due to the stabilized vertical and horizontal velocities present in an approach to landing.

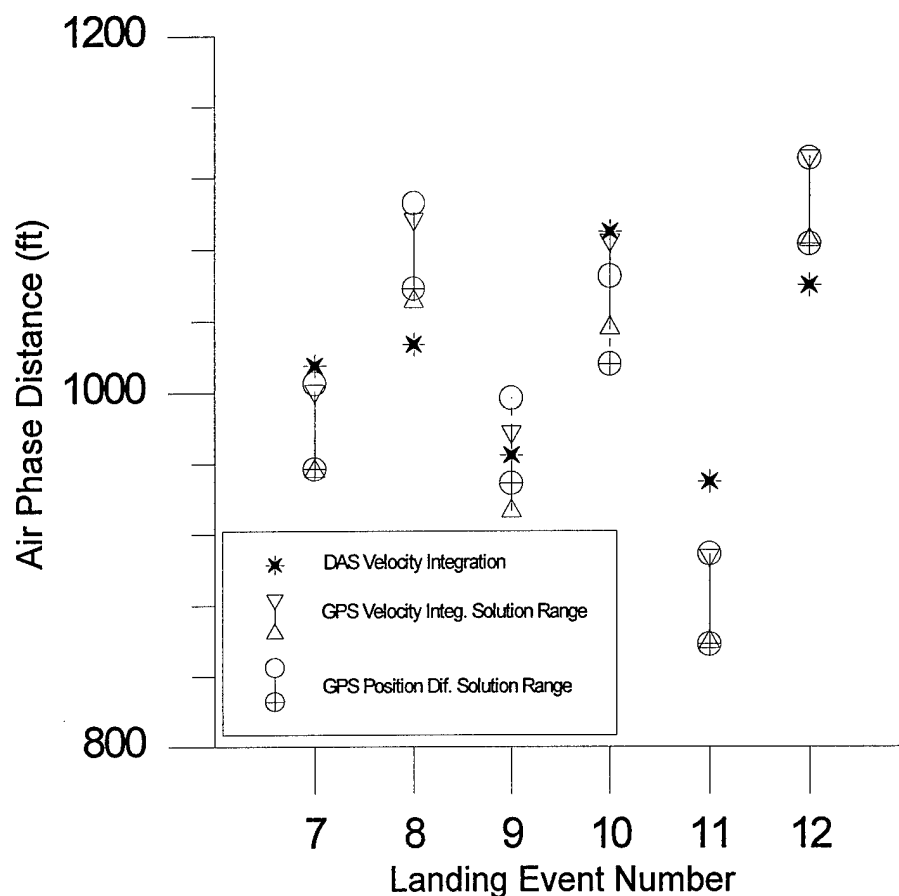


Figure 9.9: Landing Air Phase Distance Results for Flight GPS-05

Landing Ground Phase Distance Results

The ground phase of the landing is the distance covered from touchdown to full stop. Since a backward integration technique is used by the GPS algorithms, this distance is calculated first. Again, a reliable method of determining the touchdown point was not found. As a result the GPS solutions are only good to a half second range, resulting in a solution range of

approximately 50 feet. This high-low range is shown for both the GPS solution methods in figure 9.10. The video theodolite measurements and the 10 foot accuracy bounds are also shown. All the ranges for both the GPS methods are within 20 feet of the video data and most are within 10 feet. These results suggest that the methods are all equally valid for landing ground roll measurements if an adequate method of determining the touchdown point can be found.

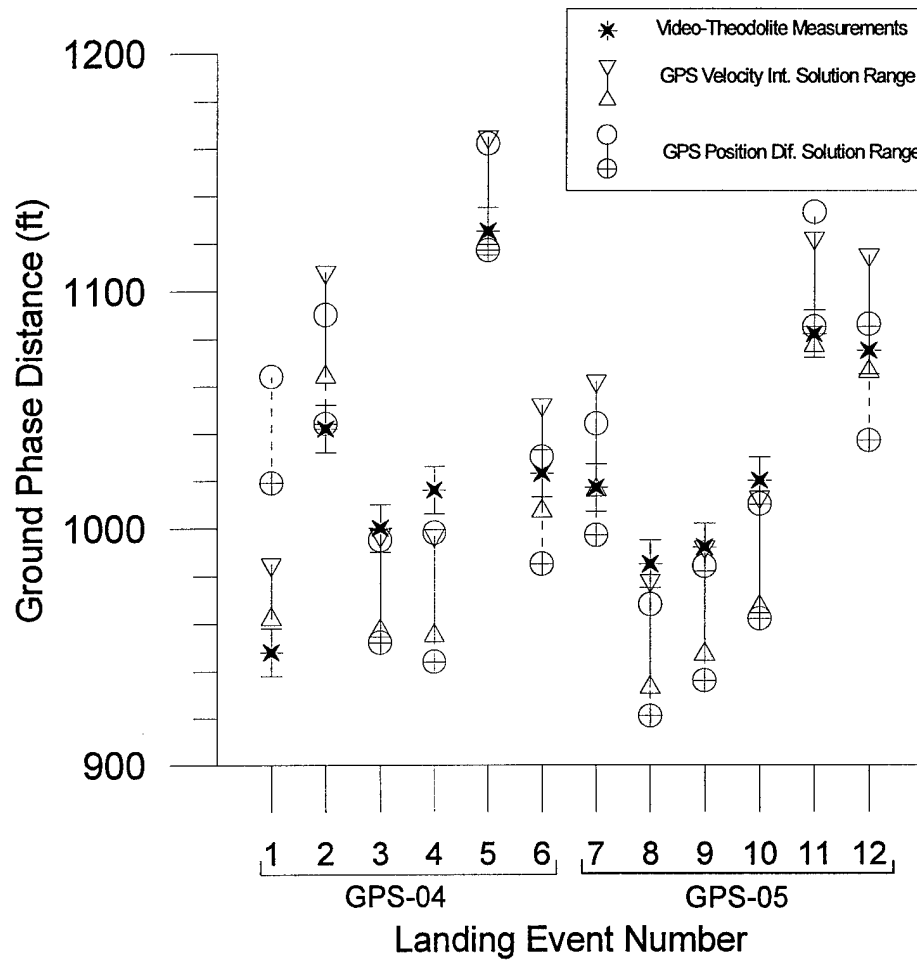


Figure 9.10: Landing Ground Phase Distance Results

Landing Position and Velocity Profiles

The distance and velocity profiles for landings are also available directly from the GPS data. Figure 9.11 shows the horizontal position and ground speed profiles for landing number 19. The vertical line marks the touchdown point in the history.

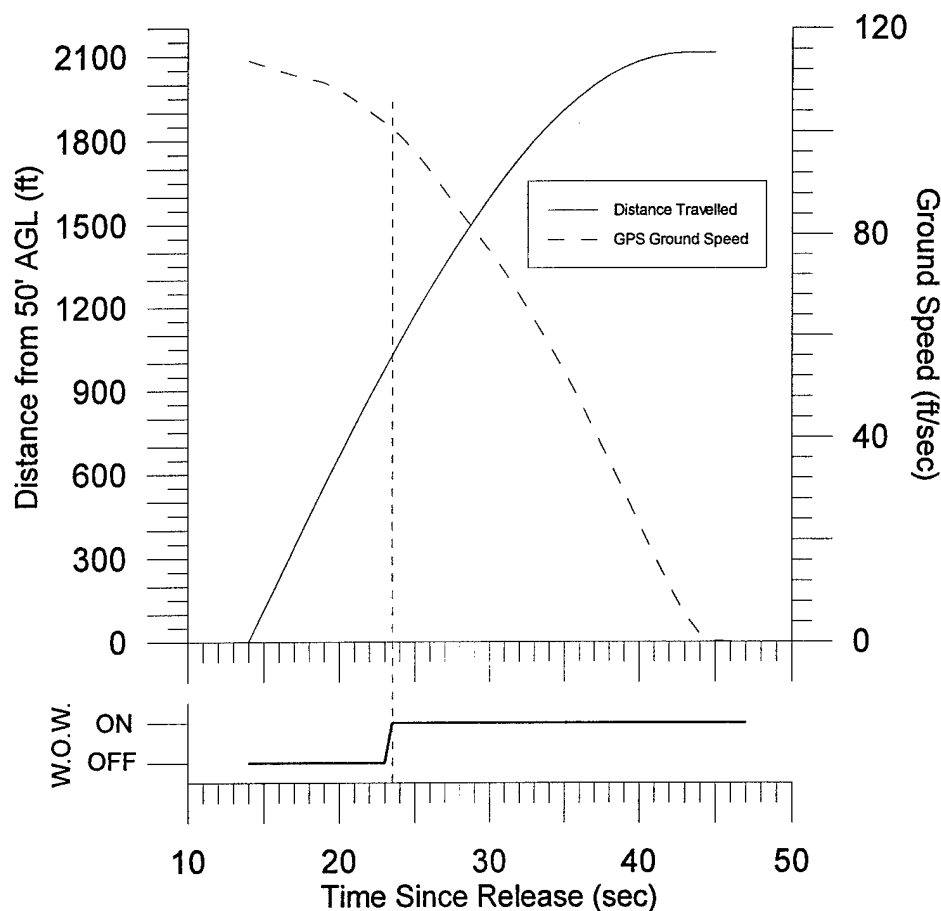


Figure 9.11: Distance and Velocity Profiles for Landing No. 11

Figure 9.12 shows the altitude and vertical velocity profiles for landing number 19. The vertical velocity appears to be noisy during the period of time leading to touchdown. Rather than noise, it is more likely that this is due to the pilot controlling the aircraft descent rate to maintain

the glidepath. It is interesting to note that the vertical descent rate decreases to zero and the altitude stops decreasing when weight on wheels occurs. There is a small amount of residual descent rate after touchdown. This is due to the negative slope of runway 18 at Starkville-Bryan field.

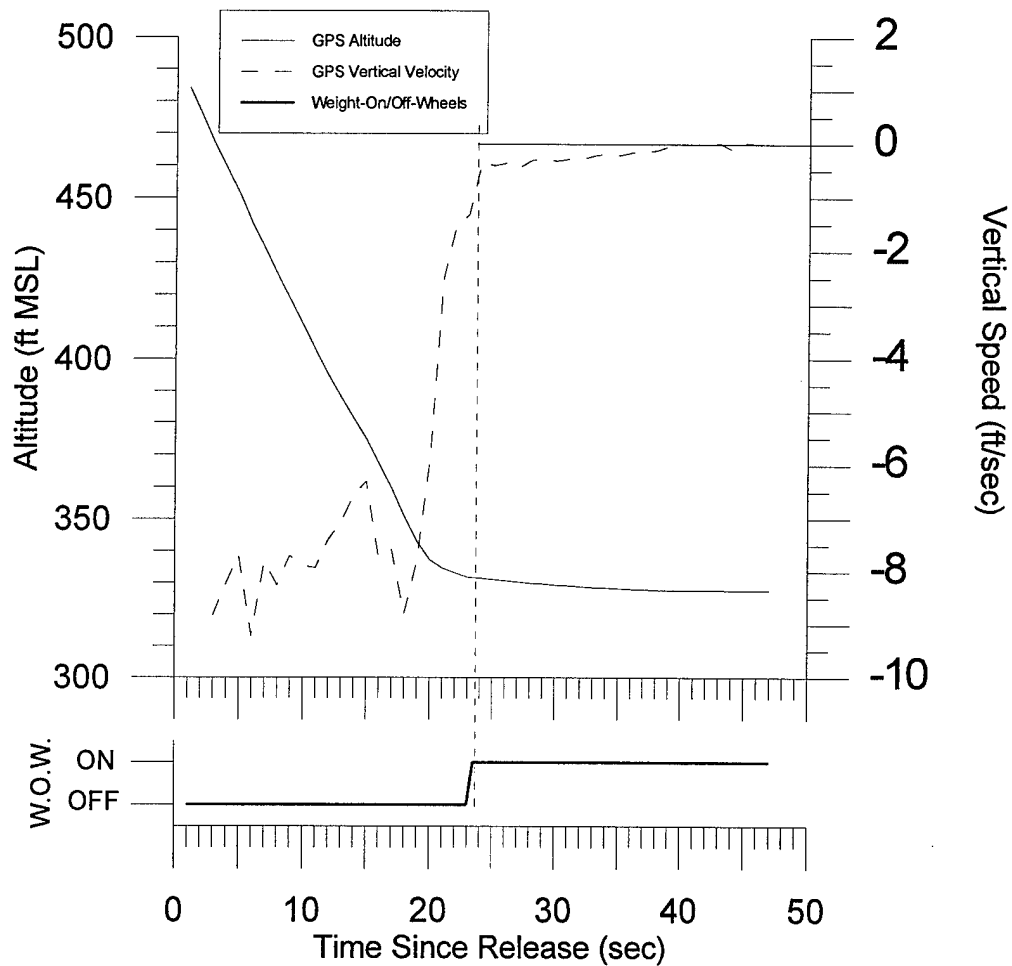


Figure 9.12: Altitude and Velocity Profiles for Landing No. 11

CHAPTER X

CONCLUSIONS AND RECOMMENDATIONS

This study demonstrates mixed results in using DGPS as a takeoff and landing theodolite. The following is a summary of these results

- 1) A time dependent position and velocity lag exists which is due to the DGPS data post-processing filter algorithm. This lag ranges from as much as 5 seconds during the first 20 minutes of a flight to .5 sec during the final 40 minutes of a flight.
- 2) For the takeoff ground roll, the DGPS velocity integration method yields results that are within the 10 feet error bounds of the traditional video theodolite measurements. This is an excellent result considering that the video-theodolite best-case accuracy is 10 feet.
- 3) The DGPS position differencing over predicts the takeoff ground phase distance. However, this appears to be due the filter algorithm introducing velocity and position time-lead errors.
- 4) The accuracy of the DGPS air phase measurements is inconclusive. This appears to be a shortcoming of using air data measurements as a reference.
- 5) The accuracy of the landing measurements is also inconclusive. This is due to an inability to determine the exact liftoff and touchdown points rather than a shortcoming of the DGPS.

The DGPS data provides good position and velocity time histories. Using the DGPS for these tests requires no support other than the flight crew. Therefore, despite the problems encountered with this first attempt at making the RFRL DGPS system work, it deserves continued attention.

Future Studies

The first logical step in improving the DGPS system for use in takeoff and landing performance testing is precise time synchronization. It is crucial that all the data sources be

exactly synchronized. Hass recommends accomplishing this with a GPS slaved time-code generator which is then used as the timing source for all data recording.⁹ This allows the liftoff and touchdown points to be determined more accurately. The time histories of position, velocity, and acceleration could then also be evaluated in direct comparison with another theodolite. The time history comparisons could be used to evaluate the source of the position and velocity errors introduced by the DGPS data post-processor.

The time lag that is present at the beginning of each flight must also be solved. One potential solution is to take 5 minutes of static data at both the beginning and end of each flight. This would allow both forward and backward processing of the data. The forward processing would provide lag-free data following the first 20 minutes of the flight. The reverse processing would provide lag-free data for all the flight except the final 20 minutes.

It is important to quantify the quality of the air phase data. This can be accomplished by utilizing another source of truth data. Other sources could include accelerometer packages or more expensive tracking devices.

There are two DGPS system advancements available from NavSymm and Premier DGPS which might improve the quality of operation of the RFRL system. First, the system can be upgraded to output DGPS data at 4 Hz. This may allow for faster DD carrier phase ambiguity resolution and resolve some of the problems. Second, the post-processor can be upgraded to operate at near real time. This too has the potential for solving some of the problems.

The takeoff and landing environment is highly dynamic. If these problems are satisfactorily solved, the system could become approved for FAA takeoff and landing flight certification of aircraft. It could be extended for use in almost any flight test application requiring inertial time space position information (TSPI) data.

REFERENCES CITED

1. Ward, Donald T. "Chapter 5: Takeoff and Landing Flight Tests", Introduction to Flight Test Engineering. Amsterdam, Netherlands: Elsevier, 1993.
2. National Test Pilot School. "Chapter 18: Takeoff and Landing", Introduction to Performance and Flying Qualities Flight Testing. Mojave, California: NTPS, 1996.
3. Trimble Navigation Ltd. All About GPS. http://www.trimble.com/gps/fsections/aa_f1.htm. Trimble Navigation Ltd., 1997.
4. United States Air Force Test Pilot School. "Chapter 8: Takeoff and Landing Performance" Performance Handbook, Vol. I. Edwards AFB, California: USAF Test Pilot School, 1993.
5. Vlegheert, J.P.K. "Performance: Takeoff and Landing Tests", Introduction to Flight Test Engineering, Quebec: AGARD, 1995.
6. Federal Aviation Regulations. PART 23--AIRWORTHINESS STANDARDS: NORMAL, UTILITY, ACROBATIC, AND COMMUTER CATEGORY AIRPLANES [_http://www.faa.gov/AVR/AFS/FARS/far-23.txt](http://www.faa.gov/AVR/AFS/FARS/far-23.txt). Washington: Federal Aviation Administration, 1997.
7. Herrington, et al. "Chapter 6: Takeoff and Landing Performance" AFTR No. 6273: Flight Test Engineering Handbook : Edwards AFB, California: Air Force Flight Test Center, 1994.
8. Erb, Russel E. "A Low Cost Method For Generating Takeoff Ground Roll Charts From Flight Test Data" Proceedings: Society of Flight Test Engineers 27th Annual International Flight Test Symposium, 11-13 November Fort Worth, Texas . : Lancaster, California: SFTE, 1996.
9. Haas, A. "Evaluation of a GPS Sensor For Runway Performance Tests" " Proceedings: Society of Flight Test Engineers 27th Annual International Flight Test Symposium, 11-13 November Fort Worth, Texas. Lancaster, California: SFTE, 1996.
10. Ffoulkes-Jones, G., Cossandier, D. "Utilizing a Low Cost GPS Receiver for Centimeter Accuracy to Sub-Meter Accuracy Real-Time and Post-Processed Applications" Proceedings of ION GPS-95: 8th International Technical Meeting of the Satellite Division of the Institute of Navigation, Sep. 12-15, 1995. Alexandria, Virginia: Institute of Navigation., 1995.

11. US Naval Observatory. NAVSTAR Global Positioning System.
<http://tycho.usno.navy.mil/gpsinfo.html>. USNO, 1996.
12. Nichols, J. W., Hammer, S. D. "Using Differential GPS As A TSPI Source in Flight Test of High Performance Aircraft" Proceedings: Society of Flight Test Engineers Silver Symposium, 1-5 Aug., 1994. Lancaster, California: SFTE, 1994.
13. Gulfstream Aerospace. AA-5B Tiger Pilots Operating Handbook.
14. Tabsh, Adel. Personal Conversation. Ontario, Canada: Premier GPS, Inc Technical Support, 2 Nov 1997.